



Giornate Nazionali EIC_NET 2024 — Bologna

27-28 June 2024

**Precision studies of QCD
in the low energy domain of the EIC:
a personal view**



Giornate Nazionali ~~EIC_NET~~ 2024 — Bologna

27-28 June 2024



Precision studies of QCD
in the low energy domain of the EIC:
a personal view

The reference paper

Precision Studies of QCD in the Low Energy Domain of the EIC

V.D. Burkert,¹ L. Elouadrhiri,¹ A. Afanasev,² J. Arrington,³ M. Contalbrigo,⁴ W. Cosyn,^{5,6} A. Deshpande,⁷ D.I. Glazier,⁸ X. Ji,^{9,10} S. Liuti,¹¹ Y. Oh,^{12,13} D. Richards,¹ T. Satogata,¹ A. Vossen,^{14,1} H. Abdolmaleki,¹⁵ A. Albataineh,¹⁶ C.A. Aidala,¹⁷ C. Alexandrou,¹⁸ H. Avagyan,¹ A. Bacchetta,¹⁹ M. Baker,¹ F. Benmokhtar,²⁰ J.C. Bernauer,^{7,21} C. Bissolotti,¹⁹ W. Briscoe,² D.Byers,¹⁴ Xu Cao,²² C.E. Carlson,²³ K. Cichy,²⁴ I.C. Cloet,²⁵ C. Cocuzza,²⁶ P.L. Cole,²⁷ M. Constantinou,²⁶ A. Courtoy,²⁸ H. Dahiya,²⁹ K. Dehmelt,⁷ S. Diehl,^{30,31} C. Dilks,¹⁴ C. Djalali,³² R. Dupré,³³ S.C. Dusa,¹ B. El-Bennich,³⁴ L. El Fassi,³⁵ T. Frederico,³⁶ A. Freese,³⁷ B.R. Gamage,¹ L. Gamberg,³⁸ R.R. Ghoshal,¹ F.X. Girod,¹ V.P. Goncalves,^{39,22,40} Y. Gotra,¹ F.K. Guo,^{41,42} X. Guo,⁹ M. Hattawy,⁴³ Y. Hatta,⁴⁴ T. Hayward,³⁰ O. Hen,⁴⁵ G. M. Huber,⁴⁶ C. Hyde,⁴³ E.L. Isupov,⁴⁷ B. Jacak,³ W. Jacobs,⁴⁸ A. Jentsch,⁴⁴ C.R. Ji,⁴⁹ S. Joosten,²⁵ N. Kalantarians,⁵⁰ Z. Kang,^{51,52,53} A. Kim,^{30,1} S. Klein,³ B. Kriesten,¹⁰ S. Kumano,⁵⁴ A. Kumar,⁵⁵ K. Kumericki,⁵⁶ M. Kuchera,⁵⁷ W.K. Lai,^{58,59,51} Jin Li,⁶⁰ Shujie Li,³ W. Li,⁶¹ X. Li,⁶² H.-W. Lin,⁶³ K.F. Liu,⁶⁴ Xiaohui Liu,^{65,66} P. Markowitz,⁵ V. Mathieu,^{67,68} M. McEneaney,¹⁴ A. Mekki,⁶⁹ J.P. B. C. de Melo,⁷⁰ Z.E. Meziani,²⁵ R. Milner,⁴⁵ H. Mkrtchyan,⁷¹ V. Mochalov,^{72,73} V. Mokeev,¹ V. Morozov,⁷⁴ H. Moutarde,⁷⁵ M. Murray,⁷⁶ S. Mtingwa,⁷⁷ P. Nadel-Turonski,⁵³ V.A. Okorokov,⁷³ E. Onyie,¹ L.L.Pappalardo,^{4,78} Z. Papandreou,⁷⁹ C. Pecar,¹⁴ A. Pilloni,^{80,81} B. Pire,⁸² N. Polys,⁸³ A. Prokudin,^{84,1} M. Przybycien,⁸⁵ J-W. Qiu,¹ M. Radici,⁸⁶ R. Reed,⁸⁷ F. Ringer,^{1,43} B.J. Roy,⁸⁸ N. Sato,¹ A. Schäfer,⁸⁹ B. Schmookler,⁹⁰ G. Schnell,⁹¹ P. Schweitzer,³⁰ R. Seidl,^{92,21} K.M. Semenov-Tian-Shansky,^{12,93,94} F. Serna,^{95,96} F. Shaban,⁹⁷ M.H. Shabestari,⁹⁸ K. Shiells,¹⁰ A. Signori,^{99,100} H. Spiesberger,¹⁰¹ I. Strakovsky,² R.S. Sufian,^{23,1} A. Szczepaniak,^{102,1} L. Teodorescu,¹⁰³ J. Terry,^{51,52} O. Teryaev,¹⁰⁴ F. Tassarotto,¹⁰⁵ C. Timmer,¹ Abdel Nasser Tawfik,¹⁰⁶ L. Valenzuela Cazares,¹⁰⁷ A. Vladimirov,^{89,108} E. Voutier,³³ D. Watts,¹⁰⁹ D. Wilson,¹¹⁰ D. Winney,^{111,112} B. Xiao,¹¹³ Z. Ye,¹¹⁴ Zh. Ye,¹¹⁵ F. Yuan,³ N. Zachariou,¹⁰⁹ I. Zahed,⁷ J.L. Zhang,⁶⁰ Y. Zhang,¹ and J. Zhou¹¹⁶

Prog. Part. Nucl. Phys. 131 (2023) 104032, arXiv:2211.15746

Motivation

from the FOREWORD:

... The goal of the initiative leading to this white paper was to take a fresh look at the changing landscape of the science underlying the need of a complementary approach towards the overall optimization and the execution of the EIC science program, and include, where appropriate, recent scientific advancements and challenges that go beyond the original motivation for the EIC. ...

- kickoff meeting (hybrid), MIT Dec. 15-16 2020 <https://indico.bnl.gov/event/9794>
- 1st workshop (online), ANL+CFNS Mar. 17-19 2021 <https://indico.bnl.gov/event/10677>
- 2nd workshop (online), APCTP+CFNS Jul. 19-23 2021 <https://indico.bnl.gov/event/11669>

Motivation

from the FOREWORD:

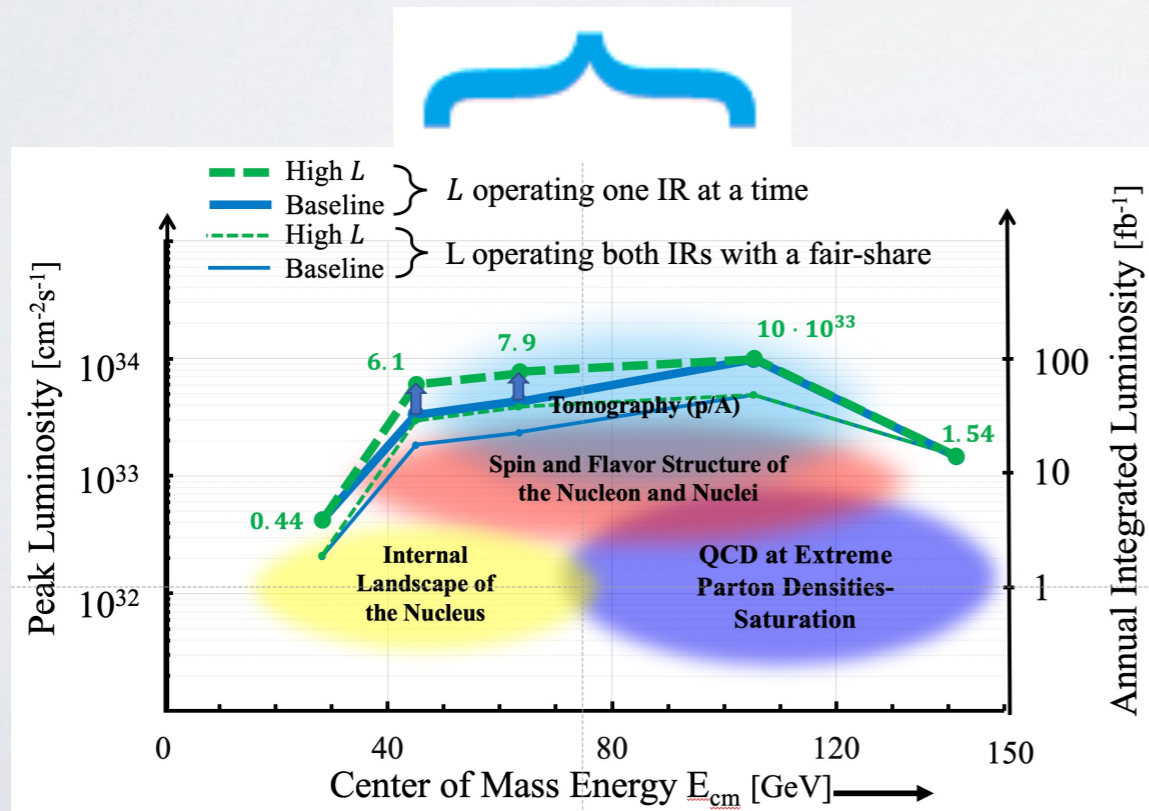
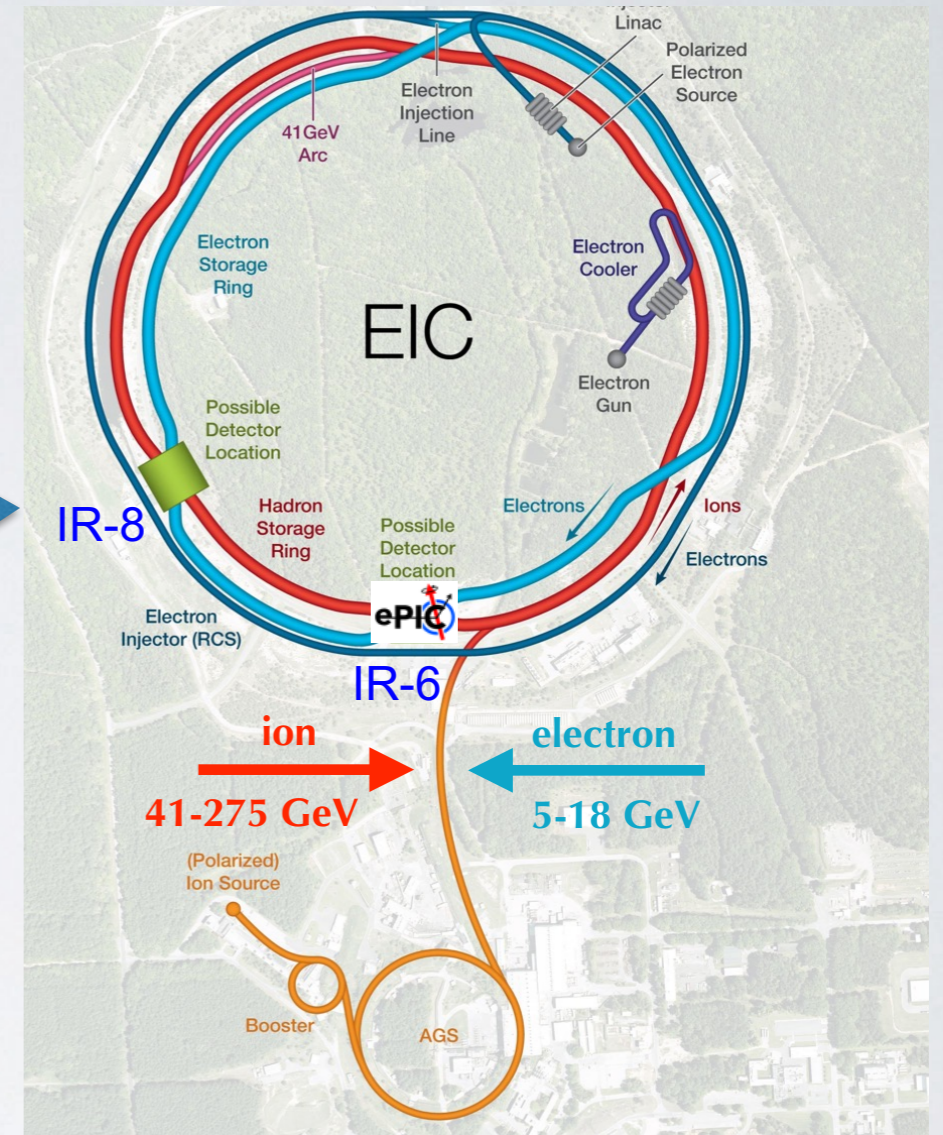
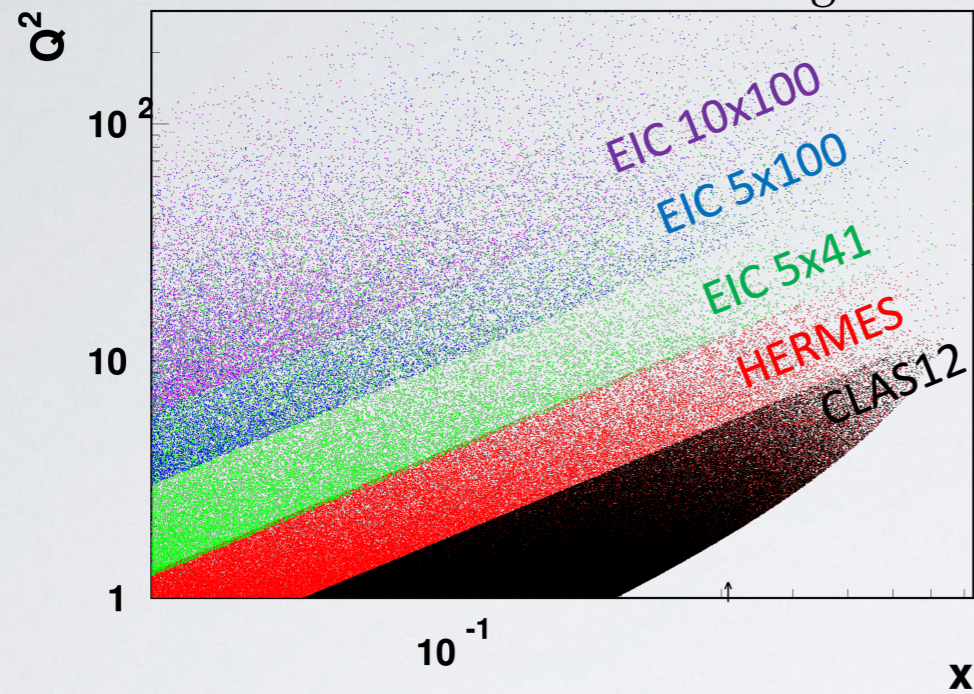
... The goal of the initiative leading to this white paper was to take a fresh look at the changing landscape of the science underlying the need of a complementary approach towards the overall optimization and the execution of the EIC science program, and include, where appropriate, recent scientific advancements and challenges that go beyond the original motivation for the EIC. ...

... It identifies part of the science program in the precision studies of QCD that require or greatly benefit from the high luminosity and low to medium center-of-mass energies, and it documents the scientific underpinnings in support of such a program. The objective of this document is to help define the path towards the realization of the second interaction region.

- kickoff meeting (hybrid), MIT Dec. 15-16 2020 <https://indico.bnl.gov/event/9794>
- 1st workshop (online), ANL+CFNS Mar. 17-19 2021 <https://indico.bnl.gov/event/10677>
- 2nd workshop (online), APCTP+CFNS Jul. 19-23 2021 <https://indico.bnl.gov/event/11669>

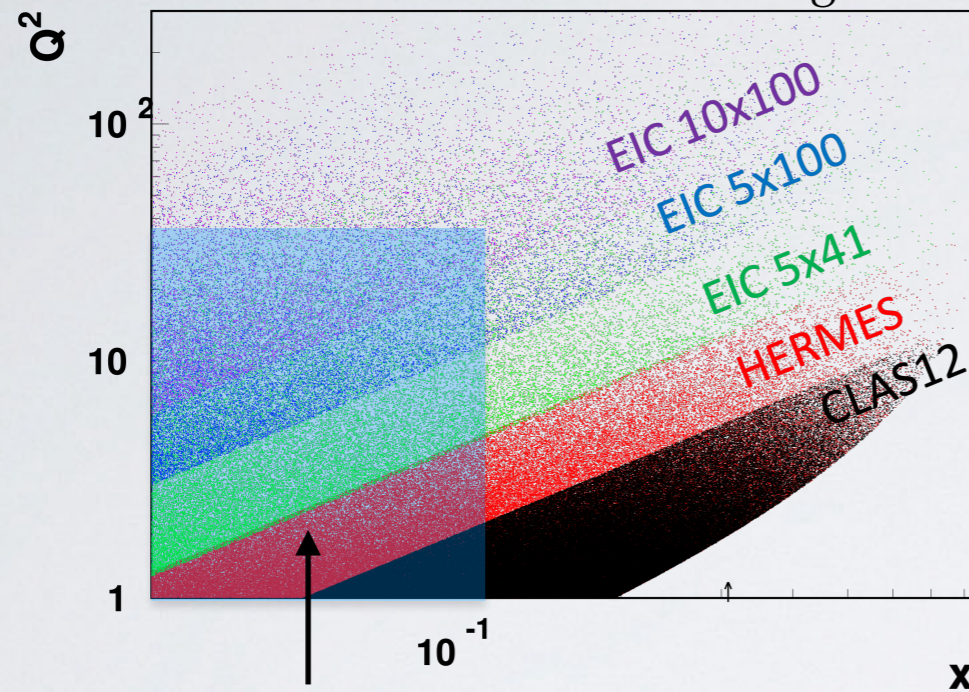
Motivation

Fig.19 of paper

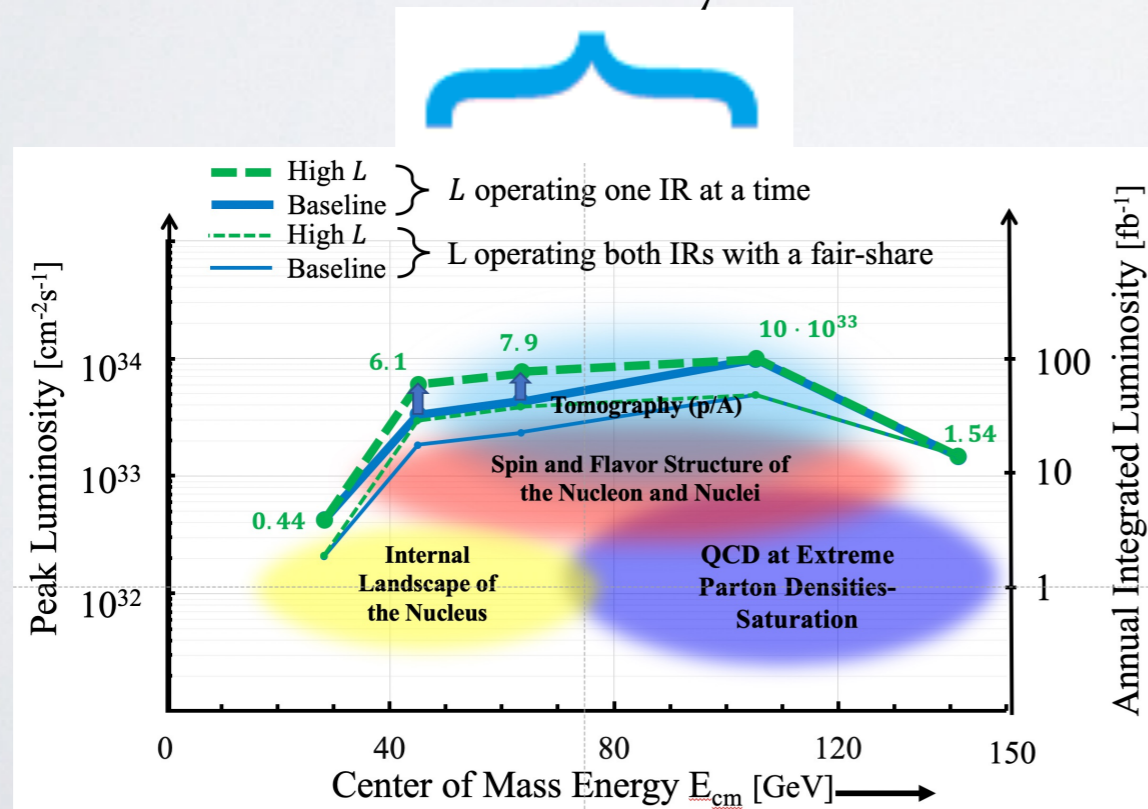
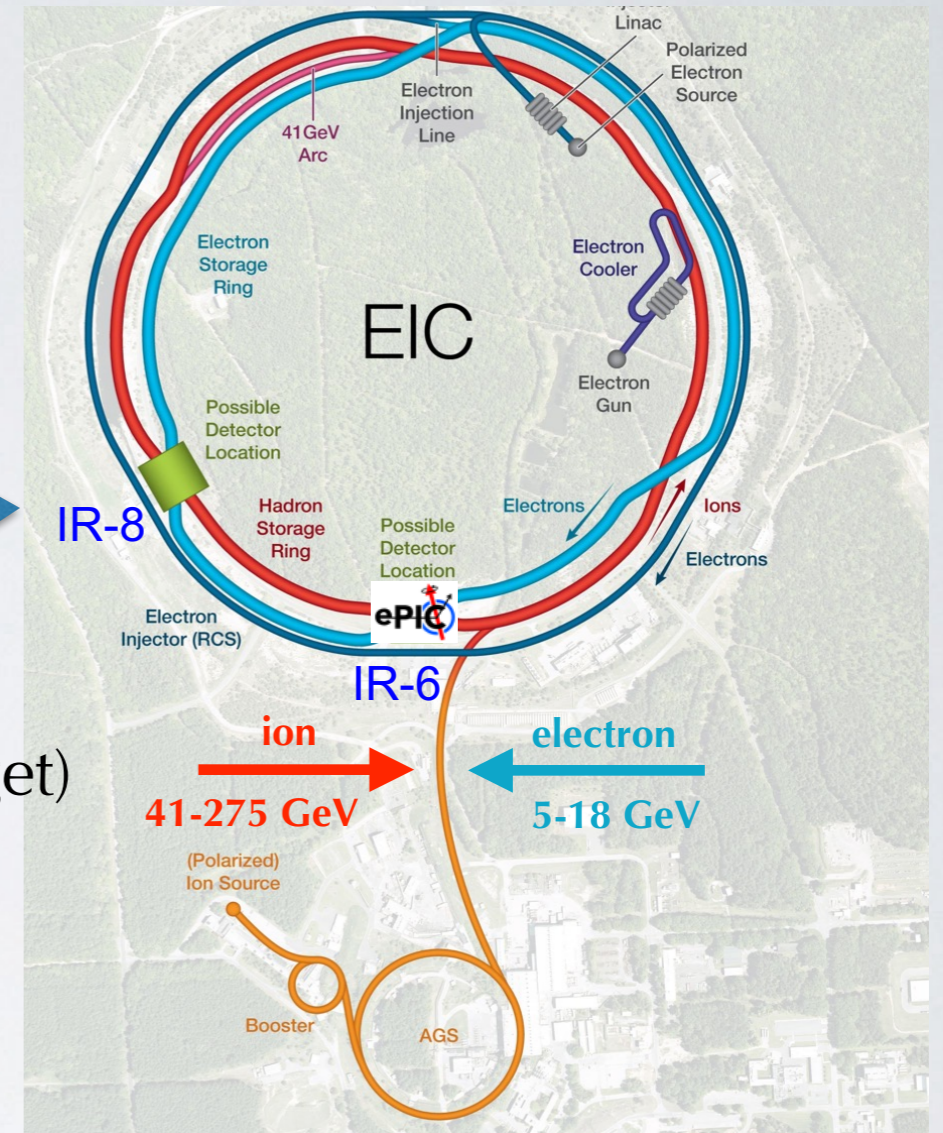


Motivation

Fig.19 of paper



area complementary to valence-like regime (fixed target) and with maximum luminosity



Outline of paper

- I. Executive Summary
- II. GPDs - 3D Imaging and mechanical properties of the nucleon
- III. Mass and spin of the nucleon
- IV. Accessing the Momentum Dependent Structure of the nucleon in Semi-Inclusive Deep Inelastic Scattering
- V. Exotic meson spectroscopy
- VI. Science highlights of light and heavy nuclei
- VII. Precision studies of Lattice QCD in the EIC era
- VIII. Science of far forward particle detection
- IX. Radiative effects and corrections
- X. Artificial Intelligence applications
- XI. The EIC interaction regions for a high impact science program with discovery potential

too many topics for a thorough overview in 30 min.

Outline of paper

- I. Executive Summary
- II. GPDs - 3D Imaging and mechanical properties of the nucleon
- III. Mass and spin of the nucleon
- IV. Accessing the Momentum Dependent Structure of the nucleon in Semi-Inclusive Deep Inelastic Scattering
- V. Exotic meson spectroscopy
- VI. Science highlights of light and heavy nuclei
- VII. Precision studies of Lattice QCD in the EIC era
- VIII. Science of far forward particle detection
- IX. Radiative effects and corrections
- X. Artificial Intelligence applications
- XI. The EIC interaction regions for a high impact science program with discovery potential

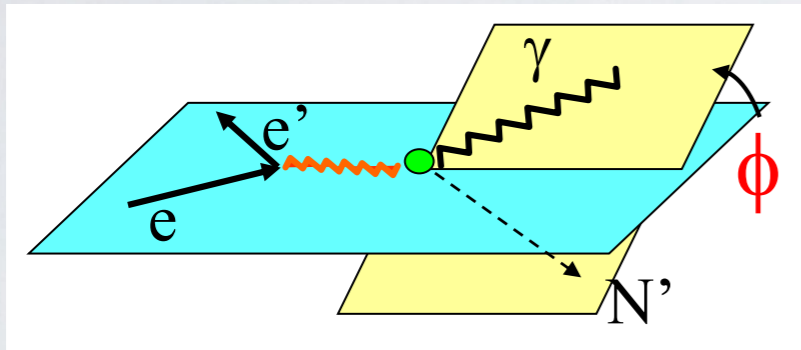
too many topics for a thorough overview in 30 min.

personal list of some top measurements

Exclusive processes

II. GPDs - 3D Imaging and mechanical properties of the nucleon

III. Mass and spin of the nucleon



Deeply Virtual Compton Scattering (DVCS)

$$d\sigma \sim \left| \text{DVCS} + \text{Bethe-Heitler} \right|^2$$

The diagram shows the mathematical expression for the differential cross-section $d\sigma$ as the squared magnitude of the sum of DVCS and Bethe-Heitler amplitudes. The DVCS amplitude is represented by a single Feynman diagram where a virtual photon is exchanged between the electron and the nucleon. The Bethe-Heitler amplitude is represented by two Feynman diagrams where the real photon is emitted from either the electron or the nucleon line. The entire sum is enclosed in large vertical bars with a superscript 2, indicating the squared magnitude of the total amplitude.

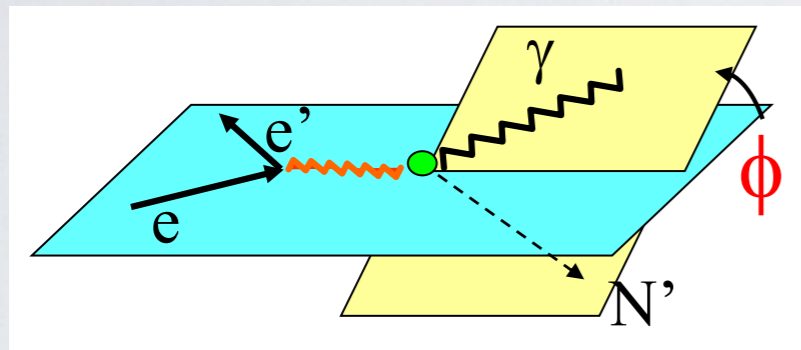
interference
of BH-DVCS
amplitudes

Exclusive processes

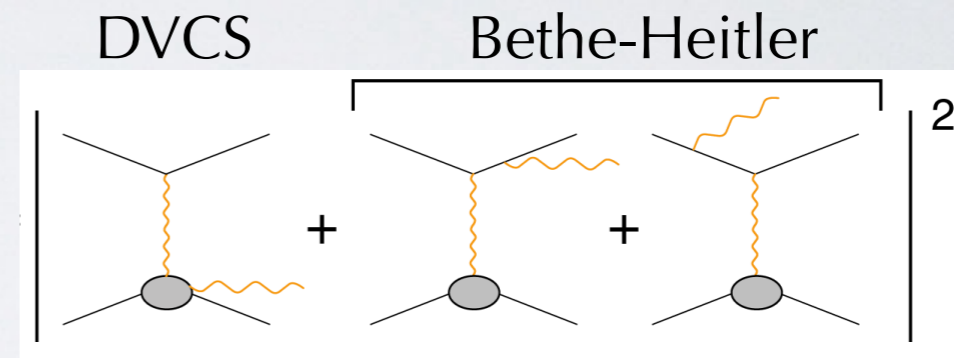
II. GPDs - 3D Imaging and mechanical properties of the nucleon

III. Mass and spin of the nucleon

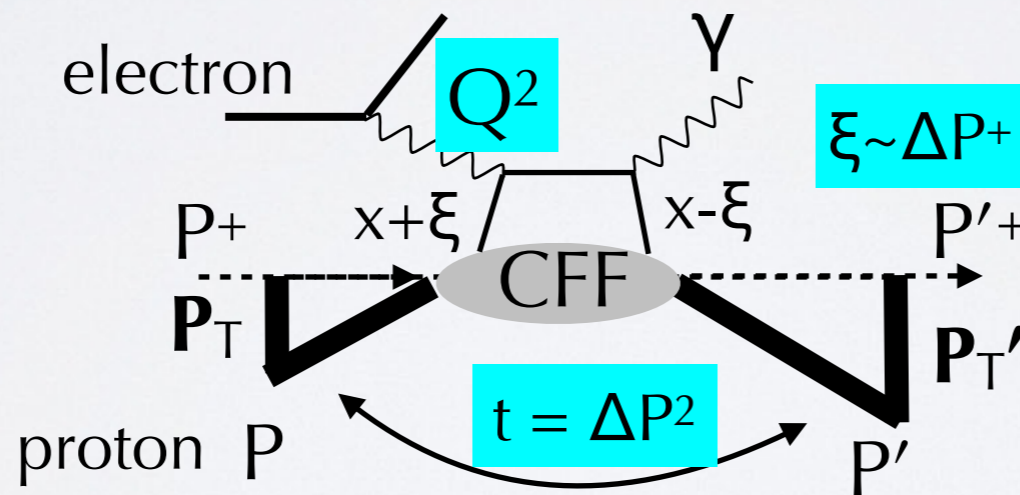
Deeply Virtual Compton Scattering (DVCS)



$$d\sigma \sim$$



interference
of BH-DVCS
amplitudes



$$\xi \sim \Delta P^+ \sim x_B / (2 - x_B)$$

$$t \ll Q^2$$

factorization of
Compton Form Factors
(CFF)

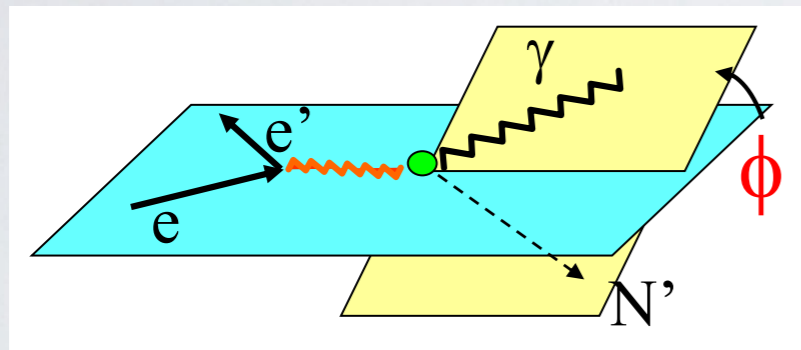
$$t = \Delta P^2$$

Exclusive processes

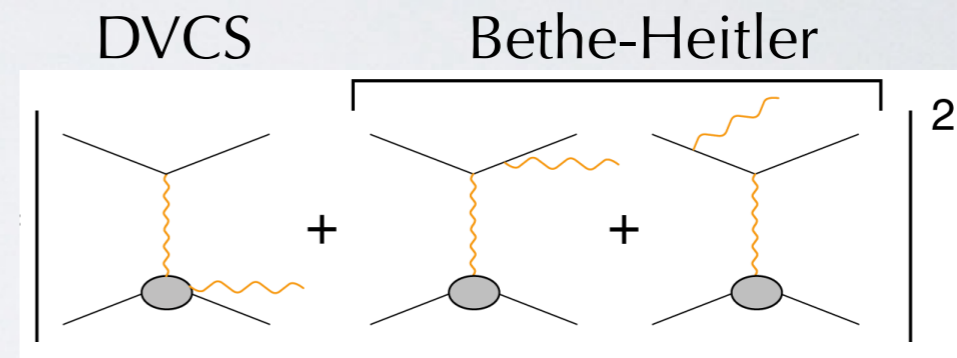
II. GPDs - 3D Imaging and mechanical properties of the nucleon

III. Mass and spin of the nucleon

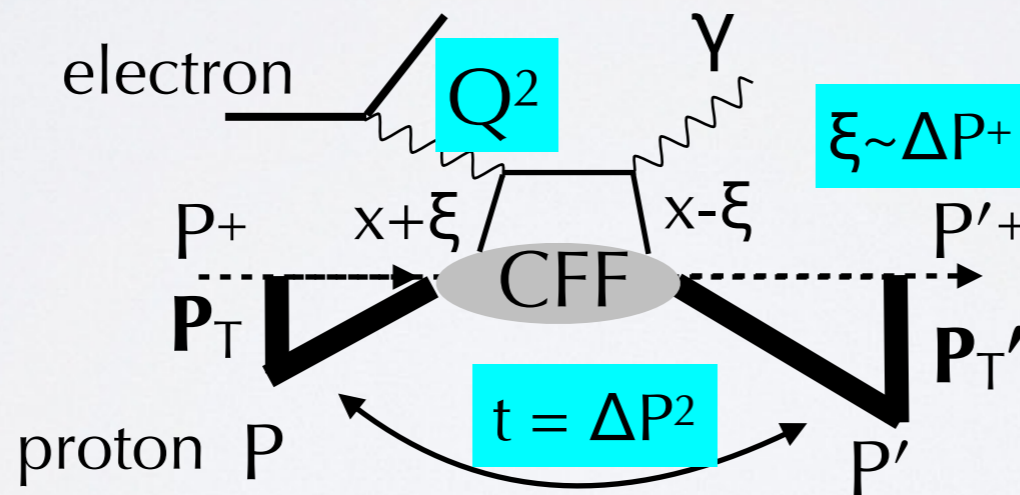
Deeply Virtual Compton Scattering (DVCS)



$$d\sigma \sim$$



interference
of BH-DVCS
amplitudes



$$\xi \sim \Delta P^+ \sim x_B / (2 - x_B)$$

$$t \ll Q^2$$

factorization of
Compton Form Factors
(CFF)

$$\text{CFF}(\xi, t) = \text{PV} \int_{-1}^1 dx \frac{\text{GPD}(x, \xi, t)}{x - \xi} - i\pi \text{GPD}(x = \pm \xi, \xi, t) + o\left(\frac{1}{Q^2}\right)$$

leading-twist GPDs

GPD are Fourier Transform of matrix elements of bilocal operators

4 structures accessible in DVCS

	operator	GPD	CFF	FF
unpol. quark •	vector $\bar{\psi}\gamma^\mu\psi$	H	\mathcal{H}	F_1
	tensor $\bar{\psi}\sigma^{\mu\nu}\Delta_\nu\psi$	E	\mathcal{E}	F_2
L-pol. quark • →	axial vector $\bar{\psi}\gamma^\mu\gamma_5\psi$	\tilde{H}	$\tilde{\mathcal{H}}$	G_A
	pseudo-scalar $\bar{\psi}\gamma_5\psi$	\tilde{E}	$\tilde{\mathcal{E}}$	G_P

flip N spin

4 additional chiral-odd structures (T-pol. quark)
accessible only in DVMP

↑

Properties of GPDs

Polynomiality (Lorentz covariance)

$$\int_{-1}^1 dx x^m \text{GPD}(x, \xi, t) = \sum_{j=0}^{\lfloor \frac{m}{2} \rfloor} \xi^{2j} C_{2j}(t) + \text{mod}(m, 2) \xi^{m+1} C_{m+1}(t)$$

Ji, J.Phys.G **24** (98) 1181
Radyushkin, P.L. **B449** (99) 81

Properties of GPDs

Polynomiality (Lorentz covariance)

$$\int_{-1}^1 dx x^m \text{GPD}(x, \xi, t) = \sum_{j=0}^{\lfloor \frac{m}{2} \rfloor} \xi^{2j} C_{2j}(t) + \text{mod}(m, 2) \xi^{m+1} C_{m+1}(t)$$

Ji, J.Phys.G **24** (98) 1181
Radyushkin, P.L. **B449** (99) 81

special cases:

$m=0 \rightarrow$ connection to form factors FF(t)

Ex.

$$\int_{-1}^1 dx H^q(x, \xi, t) = F_1^q(t)$$
$$\int_{-1}^1 dx E^q(x, \xi, t) = F_2^q(t)$$

Properties of GPDs

Polynomiality (Lorentz covariance)

$$\int_{-1}^1 dx x^m \text{GPD}(x, \xi, t) = \sum_{j=0}^{\lfloor \frac{m}{2} \rfloor} \xi^{2j} C_{2j}(t) + \text{mod}(m,2) \xi^{m+1} C_{m+1}(t)$$

Ji, J.Phys.G **24** (98) 1181
Radyushkin, P.L. **B449** (99) 81

special cases:

m=0 → connection to form factors FF(t)

Ex.

$$\int_{-1}^1 dx H^q(x, \xi, t) = F_1^q(t)$$

$$\int_{-1}^1 dx E^q(x, \xi, t) = F_2^q(t)$$

m=1 → generalized form factors → extrapolation ($t \rightarrow 0$) → mass and spin

Ex.
$$\int_{-1}^1 dx x H^q(x, \xi, t) = M^q(t) + D^q(t) \xi^2$$

$M(0)$ mass and momentum

$J(0)$ angular momentum

$$\int_{-1}^1 dx x E^q(x, \xi, t) = 2J^q(t) - M^q(t) - D^q(t) \xi^2$$

$D(0)$ “D-term” related to mechanical properties

Polyakov, P.L. **B555** (03) 57

byproduct: N spin sum rule

$$\frac{1}{2} \int_{-1}^1 dx x [H^q(x, \xi, 0) + E^q(x, \xi, 0)] = J^q$$

Ji, P.R.L. **78** (97) 610

Properties of GPDs

QCD Energy-Momentum Tensor (EMT) $T^{\mu\nu} = \bar{\psi}\gamma^\mu \frac{i}{2} \overleftrightarrow{D}^\nu \psi - F^{a\mu\lambda} F^{a\nu}{}_\lambda + \frac{1}{4} g^{\mu\nu} F^2$

$$\langle P' | T_{\mu\nu}^{q,g} | P \rangle = \bar{u}(P') \left[M^{q,g}(t) \frac{P_\mu P_\nu}{M_N} + J^{q,g}(t) \frac{i(P_\mu \sigma_{\nu\rho} + P_\nu \sigma_{\mu\rho}) \Delta^\rho}{2M_N} + D^{q,g}(t) \frac{\Delta_\mu \Delta_\nu - g_{\mu\nu} \Delta^2}{5M_N} + \bar{c}_{q,g}(t) g_{\mu\nu} \right] u(P)$$

Properties of GPDs

QCD Energy-Momentum Tensor (EMT) $T^{\mu\nu} = \bar{\psi}\gamma^\mu \frac{i}{2} \overleftrightarrow{D}^\nu \psi - F^{a\mu\lambda} F^{a\nu}{}_\lambda + \frac{1}{4} g^{\mu\nu} F^2$

$$\langle P' | T_{\mu\nu}^{q,g} | P \rangle = \bar{u}(P') \left[M^{q,g}(t) \frac{P_\mu P_\nu}{M_N} + J^{q,g}(t) \frac{i(P_\mu \sigma_{\nu\rho} + P_\nu \sigma_{\mu\rho}) \Delta^\rho}{2M_N} + D^{q,g}(t) \frac{\Delta_\mu \Delta_\nu - g_{\mu\nu} \Delta^2}{5M_N} + \bar{c}_{q,g}(t) g_{\mu\nu} \right] u(P)$$

↓
↓
↓
↓

connection to generalized form factors
 “trace anomaly”

Properties of GPDs

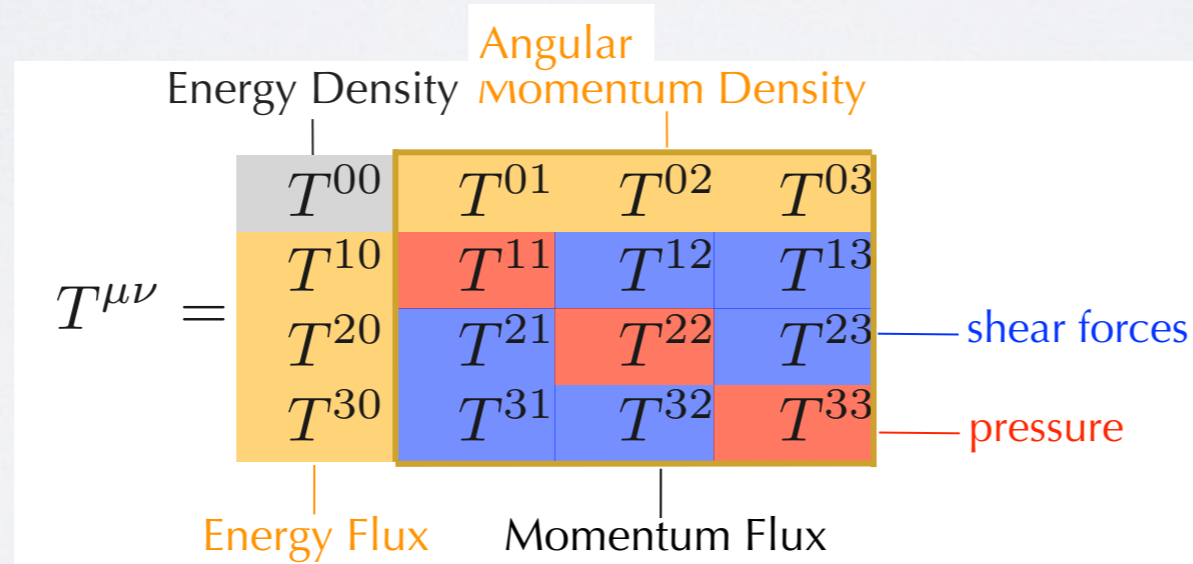
QCD Energy-Momentum Tensor (EMT) $T^{\mu\nu} = \bar{\psi}\gamma^\mu \frac{i}{2} \overleftrightarrow{D}^\nu \psi - F^{a\mu\lambda} F^{a\nu}{}_\lambda + \frac{1}{4} g^{\mu\nu} F^2$

$$\langle P' | T_{\mu\nu}^{q,g} | P \rangle = \bar{u}(P') \left[M^{q,g}(t) \frac{P_\mu P_\nu}{M_N} + J^{q,g}(t) \frac{i(P_\mu \sigma_{\nu\rho} + P_\nu \sigma_{\mu\rho}) \Delta^\rho}{2M_N} + D^{q,g}(t) \frac{\Delta_\mu \Delta_\nu - g_{\mu\nu} \Delta^2}{5M_N} + \bar{c}_{q,g}(t) g_{\mu\nu} \right] u(P)$$

↙
↓
↘
↓

connection to generalized form factors “trace anomaly”

in Breit frame ($\mathbf{\Delta} = \mathbf{P}' - \mathbf{P}$), static EMT $T_{\mu\nu}(\mathbf{r}) = \int \frac{d\Delta}{2E(2\pi)^3} e^{-i\Delta \cdot \mathbf{r}} \langle P' | T_{\mu\nu} | P \rangle \rightarrow$ probability density interpretation



Lorcé et al, P.L. **B776** (18) 38
 Lorcé et al., E.P.J. **C79** (19) 1
 Polyakov, P.L. **B555** (03) 57

Properties of GPDs

QCD Energy-Momentum Tensor (EMT) $T^{\mu\nu} = \bar{\psi}\gamma^\mu \frac{i}{2} \overleftrightarrow{D}^\nu \psi - F^{a\mu\lambda} F^{a\nu}{}_\lambda + \frac{1}{4} g^{\mu\nu} F^2$

$$\langle P' | T_{\mu\nu}^{q,g} | P \rangle = \bar{u}(P') \left[M^{q,g}(t) \frac{P_\mu P_\nu}{M_N} + J^{q,g}(t) \frac{i(P_\mu \sigma_{\nu\rho} + P_\nu \sigma_{\mu\rho}) \Delta^\rho}{2M_N} + D^{q,g}(t) \frac{\Delta_\mu \Delta_\nu - g_{\mu\nu} \Delta^2}{5M_N} + \bar{c}_{q,g}(t) g_{\mu\nu} \right] u(P)$$

connection to generalized form factors

“trace anomaly”

in Breit frame ($\mathbf{\Delta}=\mathbf{P}'-\mathbf{P}$), static EMT $T_{\mu\nu}(\mathbf{r}) = \int \frac{d\Delta}{2E(2\pi)^3} e^{-i\Delta \cdot \mathbf{r}} \langle P' | T_{\mu\nu} | P \rangle \rightarrow$ probability density interpretation

$$\int d\mathbf{r} T_{00}(\mathbf{r}) = M_N$$

	Energy Density	Angular momentum Density			
	T^{00}	T^{01}	T^{02}	T^{03}	
$T^{\mu\nu} =$	T^{10}	T^{11}	T^{12}	T^{13}	
	T^{20}	T^{21}	T^{22}	T^{23}	— shear forces
	T^{30}	T^{31}	T^{32}	T^{33}	— pressure
		Energy Flux	Momentum Flux		

Lorcé et al, P.L. **B776** (18) 38
 Lorcé et al., E.P.J. **C79** (19) 1
 Polyakov, P.L. **B555** (03) 57

Properties of GPDs

QCD Energy-Momentum Tensor (EMT) $T^{\mu\nu} = \bar{\psi}\gamma^\mu \frac{i}{2} \overleftrightarrow{D}^\nu \psi - F^{a\mu\lambda} F^{a\nu}_\lambda + \frac{1}{4} g^{\mu\nu} F^2$

$$\langle P' | T_{\mu\nu}^{q,g} | P \rangle = \bar{u}(P') \left[M^{q,g}(t) \frac{P_\mu P_\nu}{M_N} + J^{q,g}(t) \frac{i(P_\mu \sigma_{\nu\rho} + P_\nu \sigma_{\mu\rho}) \Delta^\rho}{2M_N} + D^{q,g}(t) \frac{\Delta_\mu \Delta_\nu - g_{\mu\nu} \Delta^2}{5M_N} + \bar{c}_{q,g}(t) g_{\mu\nu} \right] u(P)$$

↓
↓
↓
↓

connection to generalized form factors
“trace anomaly”

in Breit frame ($\mathbf{\Delta} = \mathbf{P}' - \mathbf{P}$), static EMT $T_{\mu\nu}(\mathbf{r}) = \int \frac{d\Delta}{2E(2\pi)^3} e^{-i\mathbf{\Delta} \cdot \mathbf{r}} \langle P' | T_{\mu\nu} | P \rangle \rightarrow$ probability density interpretation

$$\int d\mathbf{r} T_{00}(\mathbf{r}) = M_N$$

	Energy Density	Angular momentum Density			
	T^{00}	T^{01}	T^{02}	T^{03}	
$T^{\mu\nu} =$	T^{10}	T^{11}	T^{12}	T^{13}	
	T^{20}	T^{21}	T^{22}	T^{23}	— shear forces
	T^{30}	T^{31}	T^{32}	T^{33}	— pressure
		Energy Flux	Momentum Flux		

$$\int d\mathbf{r} (\mathbf{S} \times \mathbf{r})_k T_{0k}(\mathbf{r}) = 1/2$$

Lorcé et al, P.L. **B776** (18) 38
 Lorcé et al., E.P.J. **C79** (19) 1
 Polyakov, P.L. **B555** (03) 57

Properties of GPDs

QCD Energy-Momentum Tensor (EMT) $T^{\mu\nu} = \bar{\psi}\gamma^\mu \frac{i}{2} \overleftrightarrow{D}^\nu \psi - F^{\alpha\mu\lambda} F^{\alpha\nu}_\lambda + \frac{1}{4} g^{\mu\nu} F^2$

$$\langle P' | T_{\mu\nu}^{q,g} | P \rangle = \bar{u}(P') \left[M^{q,g}(t) \frac{P_\mu P_\nu}{M_N} + J^{q,g}(t) \frac{i(P_\mu \sigma_{\nu\rho} + P_\nu \sigma_{\mu\rho}) \Delta^\rho}{2M_N} + D^{q,g}(t) \frac{\Delta_\mu \Delta_\nu - g_{\mu\nu} \Delta^2}{5M_N} + \bar{c}_{q,g}(t) g_{\mu\nu} \right] u(P)$$

connection to generalized form factors

“trace anomaly”

in Breit frame ($\mathbf{\Delta} = \mathbf{P}' - \mathbf{P}$), static EMT $T_{\mu\nu}(\mathbf{r}) = \int \frac{d\Delta}{2E(2\pi)^3} e^{-i\mathbf{\Delta} \cdot \mathbf{r}} \langle P' | T_{\mu\nu} | P \rangle \rightarrow$ probability density interpretation

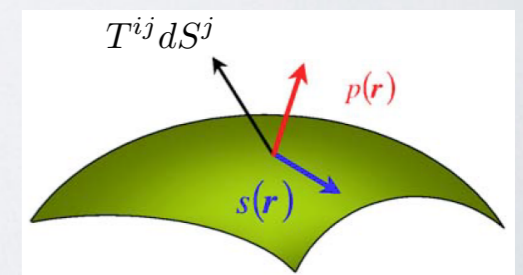
$\int d\mathbf{r} T_{00}(\mathbf{r}) = M_N$

	Energy Density	Angular momentum Density		
$T^{\mu\nu} =$	T^{00}	T^{01}	T^{02}	T^{03}
	T^{10}	T^{11}	T^{12}	T^{13}
	T^{20}	T^{21}	T^{22}	T^{23}
	T^{30}	T^{31}	T^{32}	T^{33}
	Energy Flux	Momentum Flux		

— shear forces (for $T^{12}, T^{21}, T^{13}, T^{31}, T^{23}, T^{32}$)
— pressure (for T^{11}, T^{22}, T^{33})

$\int d\mathbf{r} (\mathbf{S} \times \mathbf{r})_k T_{0k}(\mathbf{r}) = 1/2$

$T_{ij}(\mathbf{r}) = s(r) \left(\frac{r_i r_j}{r^2} - \frac{1}{3} \delta_{ij} \right) p(r) \delta_{ij}$



$D(0) = -\frac{16\pi}{15} M_N \int_0^\infty dr r^4 s(r) = 4\pi M_N \int_0^\infty dr r^4 p(r)$

D-term related to internal forces

Lorcé et al, P.L. **B776** (18) 38
Lorcé et al., E.P.J. **C79** (19) 1
Polyakov, P.L. **B555** (03) 57

Attempts of Femtography

Probability density distribution in impact parameter space

$$q(x, \mathbf{b}_\perp) = \int \frac{d\Delta_\perp}{(2\pi)^2} e^{i\Delta_\perp \cdot \mathbf{b}_\perp} H^q(x, 0, -\Delta_\perp^2) \quad \text{Burkardt, P.R. D62 (00) 071503}$$

↑
extrapolation of data to $\xi \sim \Delta P^+ = 0$

$$\langle \mathbf{b}_\perp^2(x) \rangle = \frac{\int d\mathbf{b}_\perp \mathbf{b}_\perp^2 q(x, \mathbf{b}_\perp)}{\int d\mathbf{b}_\perp q(x, \mathbf{b}_\perp)}$$

Attempts of Femtography

Probability density distribution in impact parameter space

$$q(x, \mathbf{b}_\perp) = \int \frac{d\Delta_\perp}{(2\pi)^2} e^{i\Delta_\perp \cdot \mathbf{b}_\perp} H^q(x, 0, -\Delta_\perp^2)$$

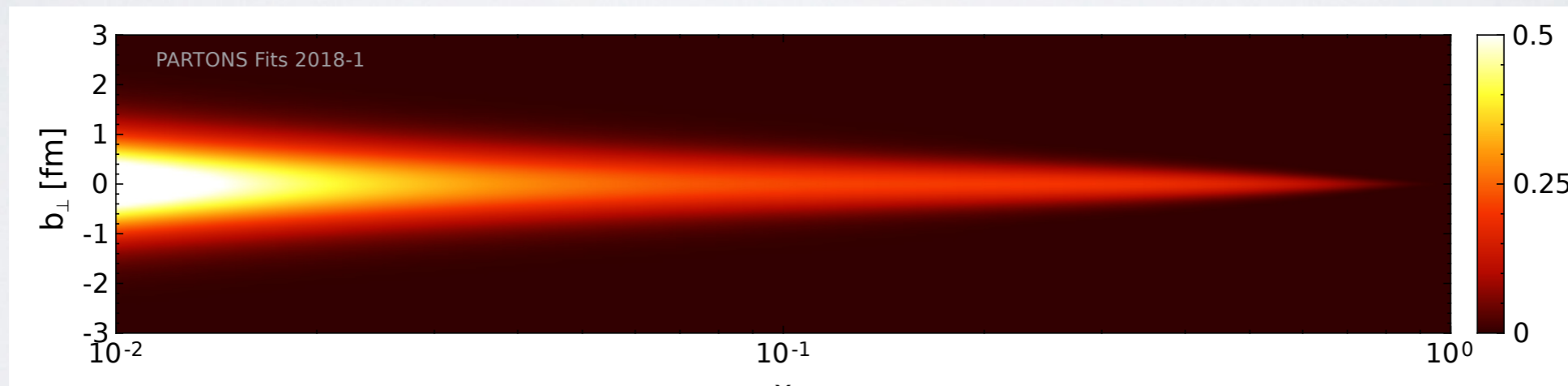
Burkardt, P.R. D62 (00) 071503

↑
extrapolation of data to $\xi \sim \Delta P^+ = 0$

fitting H^q to CLAS6
and HERMES data

$$\langle \mathbf{b}_\perp^2(x) \rangle = \frac{\int d\mathbf{b}_\perp \mathbf{b}_\perp^2 q(x, \mathbf{b}_\perp)}{\int d\mathbf{b}_\perp q(x, \mathbf{b}_\perp)}$$

Moutarde et al., E.P.J. C78 (18) 890



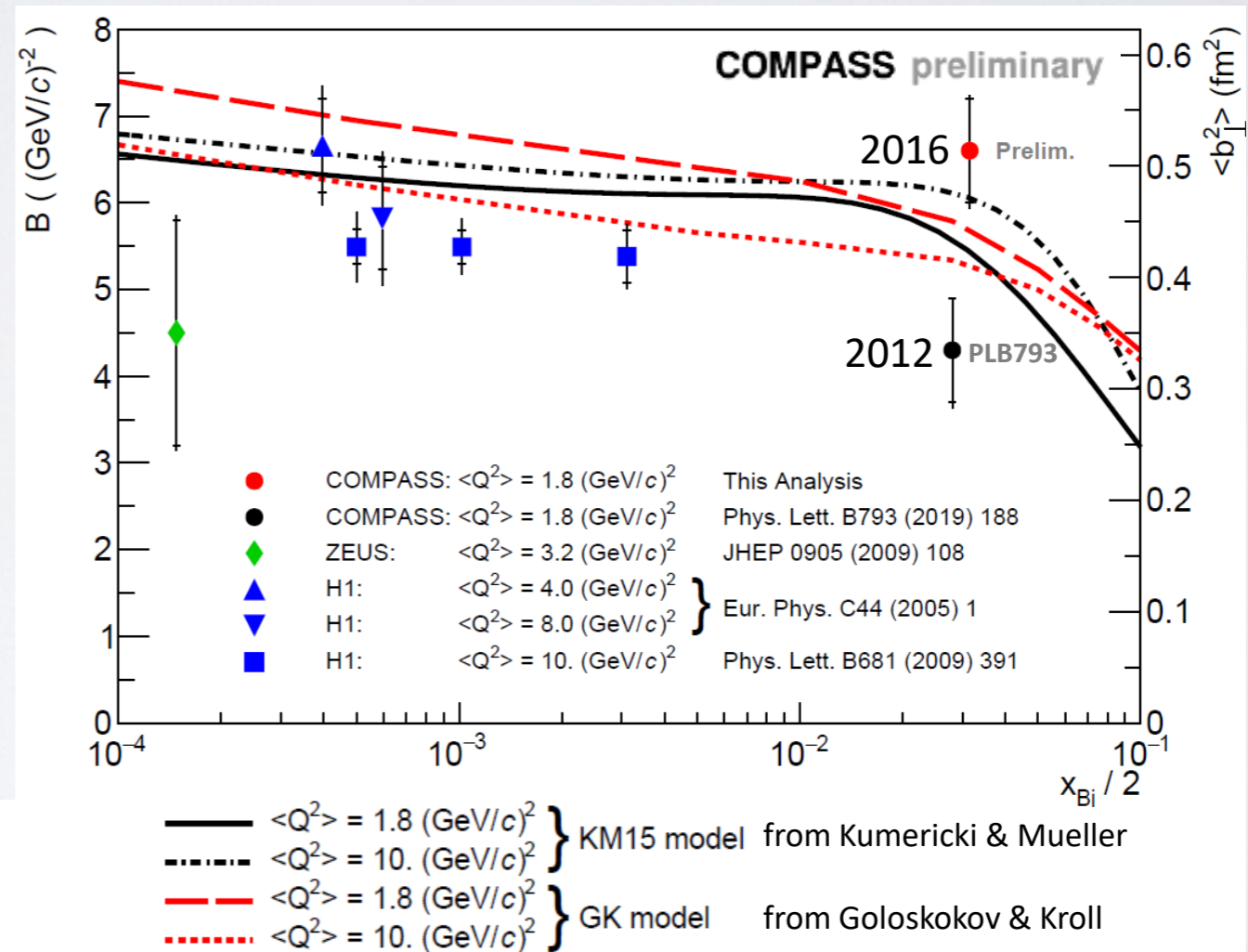
high-momentum (valence) quarks are at the core of the nucleon,
low-momentum (sea) quarks spread to its periphery

Attempts of Femtography

latest from COMPASS: $\frac{d\sigma^{\text{DVCS}}}{dt} \sim (\text{Im}[\mathcal{H}(\xi, \xi, t)])^2 \leftrightarrow e^{-B(\xi)} |t|$

$x = \xi \approx x_B/2$ small \rightarrow "extrapolation" to $\xi = 0$

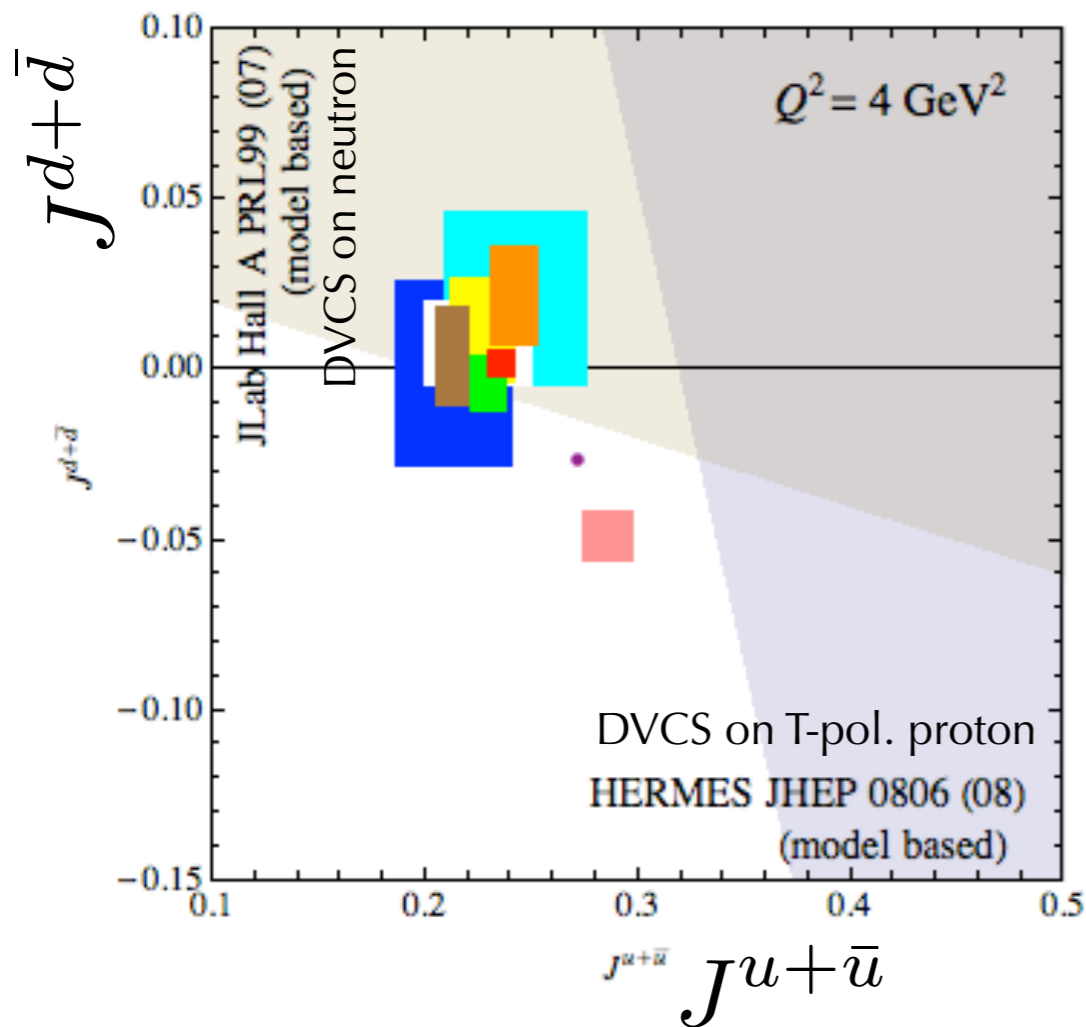
$\langle \mathbf{b}_\perp^2(x) \rangle \approx 2 B(\xi)$



2012 statistics = Ref
 2016 analysed statistics = 2.3 × Ref
 2016+2017 expected statistics = 10 × Ref

Angular momentum

$$J^q = \frac{1}{2} \int_{-1}^1 dx x [H^q(x, \xi, 0) + E^q(x, \xi, 0)]$$



- Goloskokov & Kroll, EPJ C59 (09) 809
- Kroll, QCD-N'12
- Diehl et al., EPJ C39 (05) 1
- Guidal et al., PR D72 (05) 054013
- Liuti et al., PRD 84 (11) 034007
- Bacchetta & Radici, PRL 107 (11) 212001
- LHPC-1, PR D77 (08) 094502
- LHPC-2, PR D82 (10) 094502
- QCDSF, arXiv:0710.1534
- Wakamatsu, EPJ A44 (10) 297

models
of
GPD

color lensing
Sivers \leftrightarrow E

lattice

$$J^{u-\bar{u}} = 0.214^{+0.009}_{-0.013} \quad J^{d-\bar{d}} = -0.029^{+0.021}_{-0.008}$$

$$J^{u-\bar{u}} = 0.230^{+0.009}_{-0.024} \quad J^{d-\bar{d}} = -0.004^{+0.010}_{-0.016}$$



D-term and N internal forces

D-term from
GPDs H and E

$$\int_{-1}^1 dx x H^q(x, \xi, t) = M^q(t) + D^q(t) \xi^2$$
$$\int_{-1}^1 dx x E^q(x, \xi, t) = 2J^q(t) - M^q(t) - D^q(t) \xi^2$$

but GPDs are “buried”
inside CFF \mathcal{H} , \mathcal{E}

D-term and N internal forces

D-term from GPDs H and E

$$\int_{-1}^1 dx x H^q(x, \xi, t) = M^q(t) + D^q(t) \xi^2$$
$$\int_{-1}^1 dx x E^q(x, \xi, t) = 2J^q(t) - M^q(t) - D^q(t) \xi^2$$

but GPDs are “buried” inside CFF \mathcal{H} , \mathcal{E}

DVCS: BSA data $\rightarrow \text{Im}[\mathcal{H}]$, unpol. $d\sigma^0 \rightarrow \text{Re}[\mathcal{H}]$

dispersion relations: $\text{Re}[\mathcal{H}(\xi, t, Q^2)] = \frac{1}{\pi} \text{PV} \int dx \left(\frac{1}{\xi - x} - \frac{1}{\xi + x} \right) \text{Im}[\mathcal{H}(x, t, Q^2)] - \Delta(t, Q^2)$

$$\Delta(t, Q^2) = 4 \sum_q e_q^2 \left[d_1^q(t, Q^2) + d_3^q(t, Q^2) + d_5^q(t, Q^2) + \dots \right] \approx \frac{25}{18} \sum_q D^q(t)$$

D-term and N internal forces

D-term from GPDs H and E

$$\int_{-1}^1 dx x H^q(x, \xi, t) = M^q(t) + D^q(t) \xi^2$$

$$\int_{-1}^1 dx x E^q(x, \xi, t) = 2J^q(t) - M^q(t) - D^q(t) \xi^2$$

but GPDs are “buried” inside CFF \mathcal{H}, \mathcal{E}

DVCS: BSA data $\rightarrow \text{Im}[\mathcal{H}]$, unpol. $d\sigma^0 \rightarrow \text{Re}[\mathcal{H}]$

dispersion relations: $\text{Re}[\mathcal{H}(\xi, t, Q^2)] = \frac{1}{\pi} \text{PV} \int dx \left(\frac{1}{\xi - x} - \frac{1}{\xi + x} \right) \text{Im}[\mathcal{H}(x, t, Q^2)] - \Delta(t, Q^2)$

$$\Delta(t, Q^2) = 4 \sum_q e_q^2 \left[d_1^q(t, Q^2) + d_3^q(t, Q^2) + d_5^q(t, Q^2) + \dots \right] \approx \frac{25}{18} \sum_q D^q(t)$$

$Q^2 \rightarrow \infty$

$\frac{4}{5} d_1(t) = D(t)$

0 0

Anikin & Teraev, P.R.D 76 (07) 056007

D-term and N internal forces

D-term from GPDs H and E

$$\int_{-1}^1 dx x H^q(x, \xi, t) = M^q(t) + D^q(t) \xi^2$$

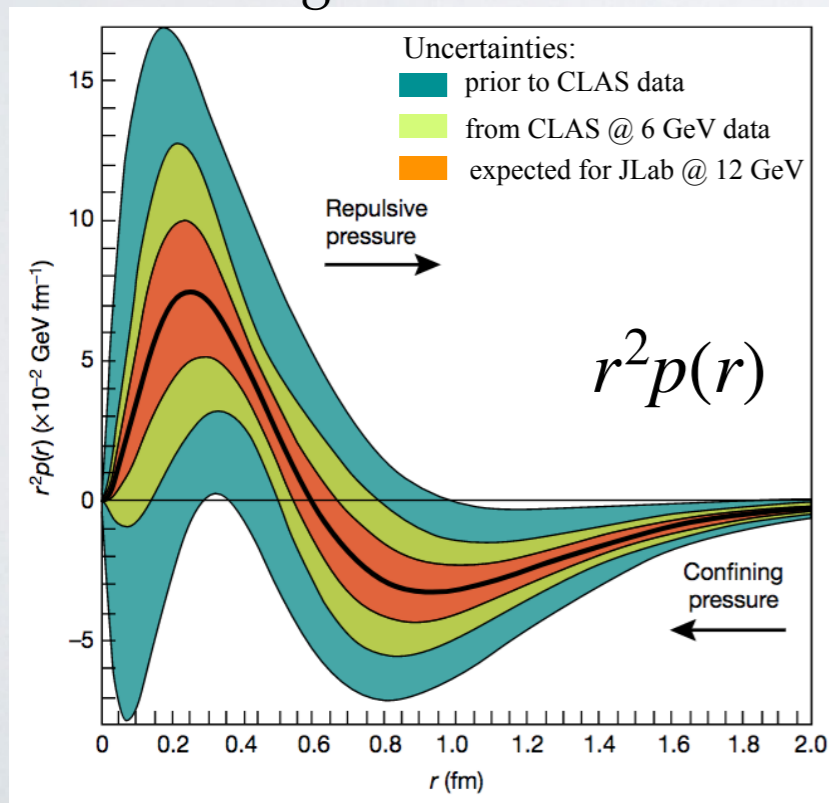
$$\int_{-1}^1 dx x E^q(x, \xi, t) = 2J^q(t) - M^q(t) - D^q(t) \xi^2$$

but GPDs are “buried” inside CFF \mathcal{H}, \mathcal{E}

DVCS: BSA data $\rightarrow \text{Im}[\mathcal{H}]$, unpol. $d\sigma^0 \rightarrow \text{Re}[\mathcal{H}]$

dispersion relations: $\text{Re}[\mathcal{H}(\xi, t, Q^2)] = \frac{1}{\pi} \text{PV} \int dx \left(\frac{1}{\xi - x} - \frac{1}{\xi + x} \right) \text{Im}[\mathcal{H}(x, t, Q^2)] - \Delta(t, Q^2)$

using CLAS6 data



Girod et al., Nature **557** (18) 7705

$$\Delta(t, Q^2) = 4 \sum_q e_q^2 \left[d_1^q(t, Q^2) + d_3^q(t, Q^2) + d_5^q(t, Q^2) + \dots \right] \approx \frac{25}{18} \sum_q D^q(t)$$

$Q^2 \rightarrow \infty$

$\frac{4}{5} d_1(t) = D(t)$

0 0

Anikin & Teraev, P.R.D **76** (07) 056007

stability

$$\int_0^\infty dr r^2 p(r) = 0$$

$$D(0) = 4\pi M_N \int_0^\infty dr r^4 p(r) < 0$$

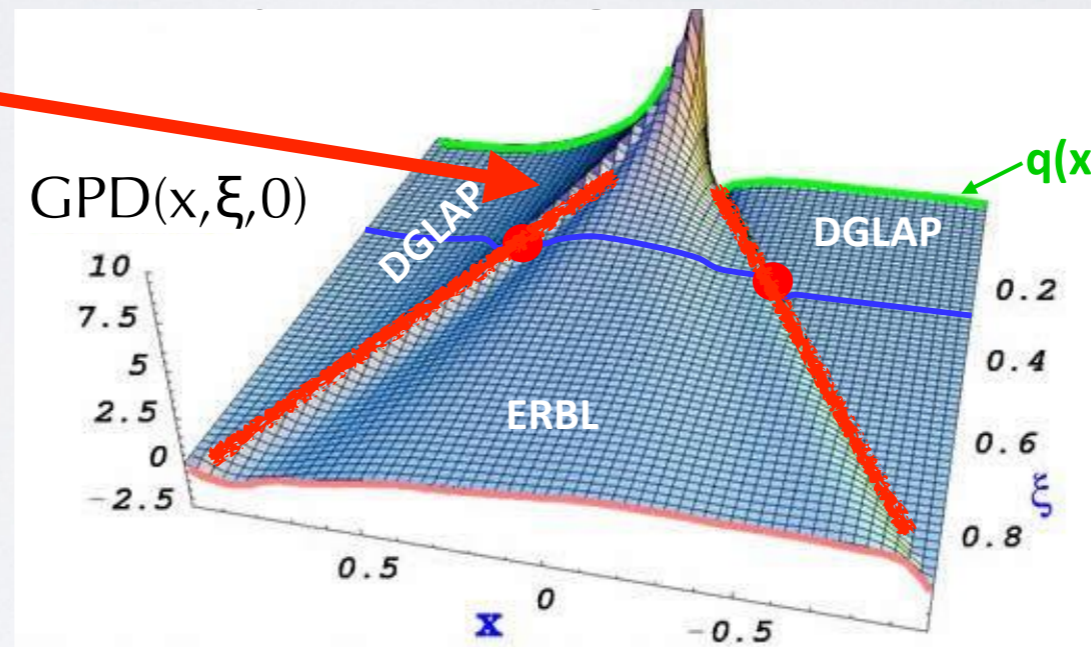
Perevalova et al., P.R.D **94** (16) 054024

consistent with data & models

Exclusive processes

$$\text{CFF}(\xi, t) = \underbrace{\text{PV} \int_{-1}^1 dx \frac{\text{GPD}(x, \xi, t)}{x - \xi}}_{\text{Re(CFF)}} - \underbrace{i\pi \text{GPD}(x = \pm \xi, \xi, t)}_{\text{Im(CFF)}} + o\left(\frac{1}{Q^2}\right)$$

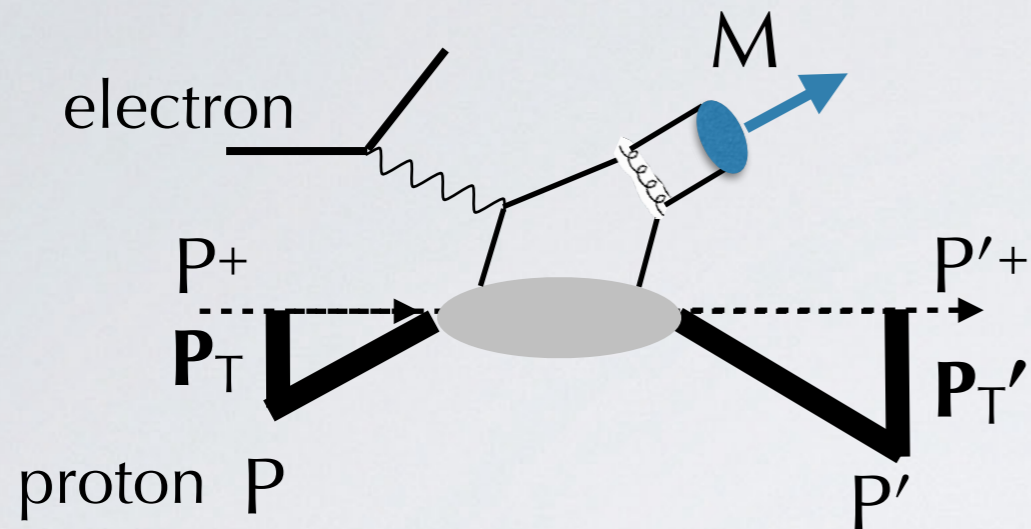
Access only to the
 $(x = \pm \xi, \xi, t)$ dependence



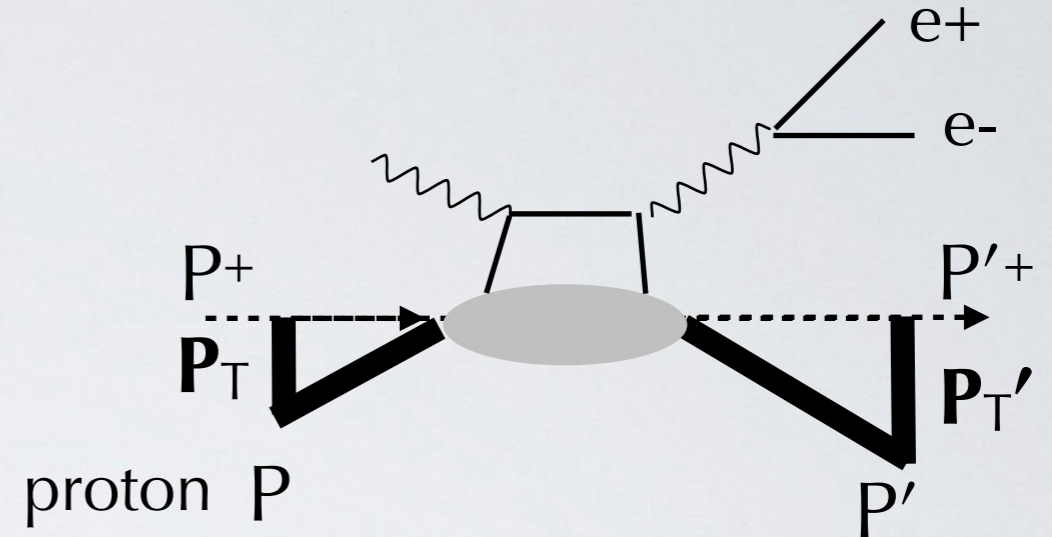
$$\text{GPD}(x, 0, 0) = \text{PDF}(x)$$

- Need to combine information from
- different DVCS measurement
 - different processes

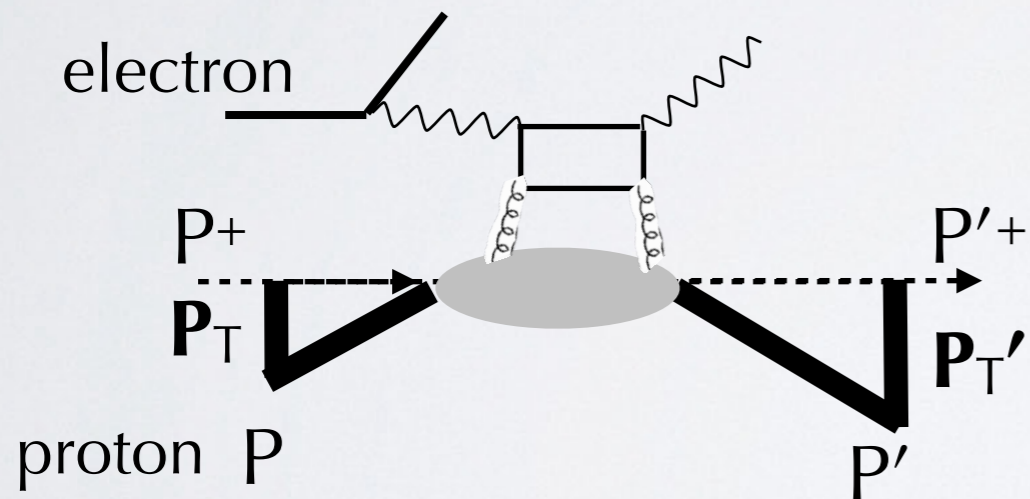
Exclusive processes



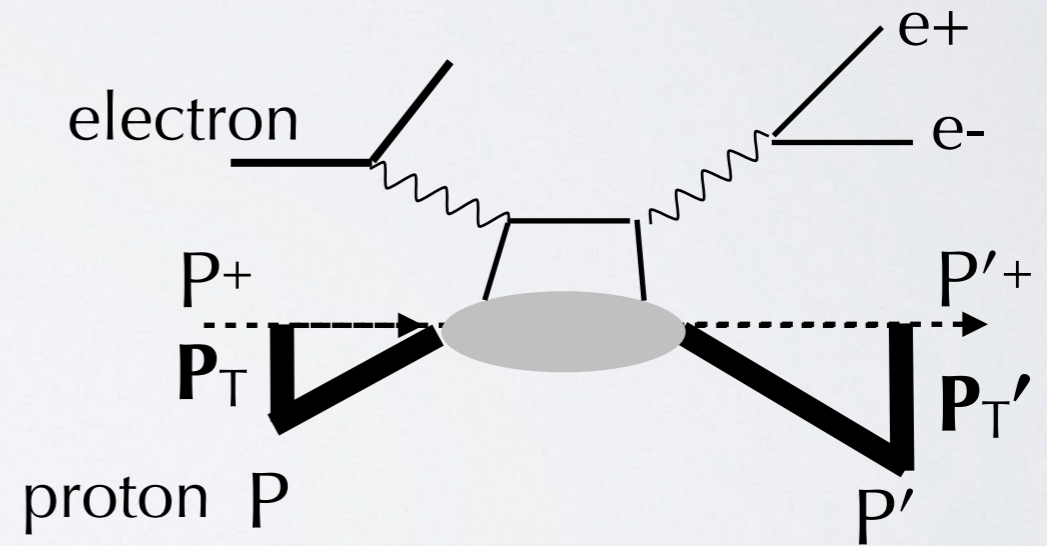
Deeply Virtual Meson Production (**DVMP**)
(access to transversity GPD)



Time-like Compton Scattering (**TCS**)
(sensitive to D-term via $\text{Re}[\mathcal{H}]$)



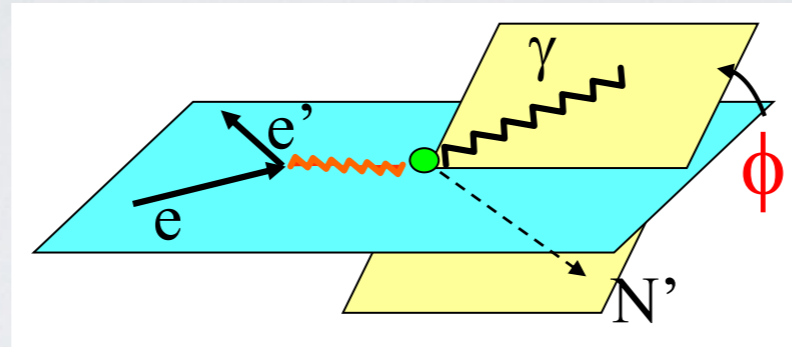
gluon channel of **DVCS**
($\rightarrow \mathcal{O}(\alpha_s)$ corrections)



Double DVCS (**DDVCS**)
(go beyond $x = \pm \xi$ limitation)

reactions ($\gamma^* N \rightarrow N' M$, $\gamma N \rightarrow N' \gamma^*$) in backward kin. ($|u| \ll s, t$)
 \rightarrow Transition Distribution Amplitudes (TDA)

CFF combinations in DVCS



polarized beam
unpol. target

$$\text{BSA } \Delta\sigma_{\text{LU}} \sim \sin\phi f \left[\text{Im}[\mathcal{H}], \text{Im}[\tilde{\mathcal{H}}], \text{Im}[\mathcal{E}] \right]$$

unpol. beam
L-pol. target

$$\ell\text{TSA } \Delta\sigma_{\text{UL}} \sim \sin\phi f \left[\text{Im}[\mathcal{H}], \text{Im}[\tilde{\mathcal{H}}], \text{Im}[\mathcal{E}], \text{Im}[\tilde{\mathcal{E}}] \right]$$

polarized beam
L-pol. target

$$\text{DSA } \Delta\sigma_{\text{LL}} \sim (A + B \cos\phi) f \left[\text{Re}[\mathcal{H}], \text{Re}[\tilde{\mathcal{H}}], \text{Re}[\mathcal{E}] \right]$$

unpol. beam
T-pol. target

$$\text{tTSA } \Delta\sigma_{\text{UT}} \sim \cos\phi \sin(\phi_S - \phi) f \left[\text{Im}[\mathcal{H}], \text{Im}[\mathcal{E}] \right]$$

unpol. beam
different charges
unpol. target

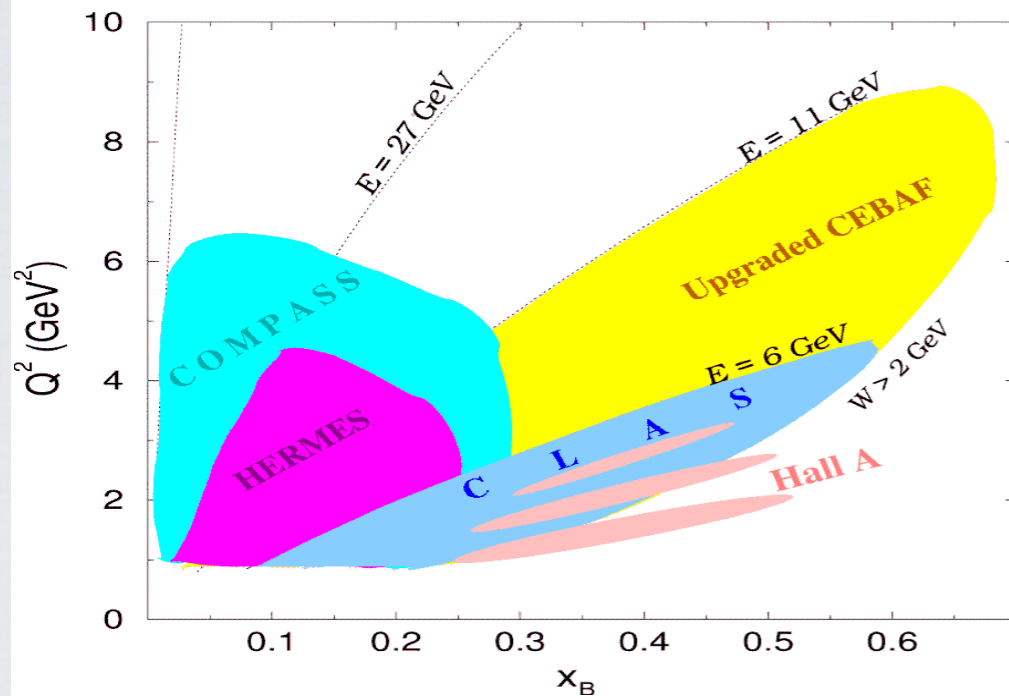
$$\text{BCA } \Delta\sigma_{\text{c}} \sim \cos\phi f \left[\text{Re}[\mathcal{H}], \text{Re}[\tilde{\mathcal{H}}], \text{Re}[\mathcal{E}] \right]$$

History of DVCS exp.'s

JLAB	
<i>Hall A</i>	<i>CLAS (Hall B)</i>
p,n-DVCS, Beam-pol. CS	p-DVCS, BSA, ITSA, DSA, CS

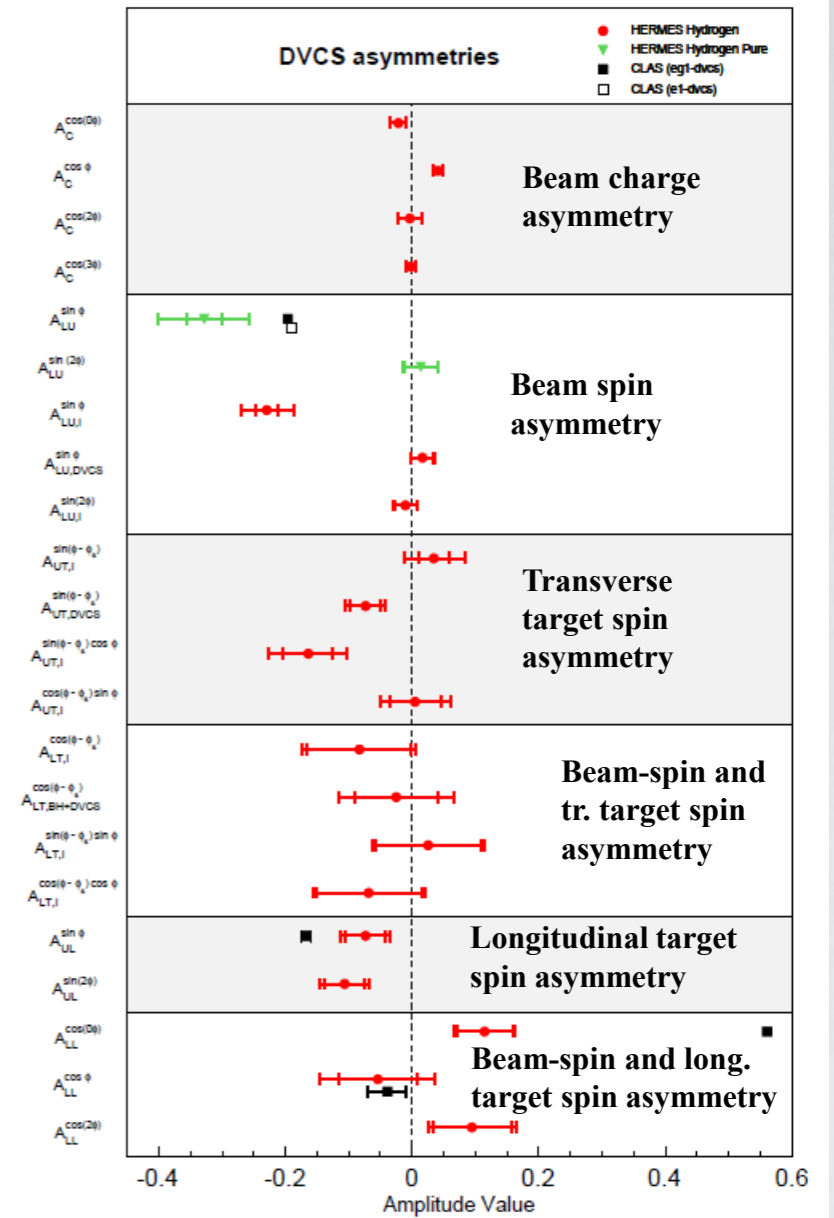
DESY	
<i>HERMES</i>	<i>H1/ZEUS</i>
p-DVCS, BSA, BCA, tTSA, ITSA, DSA	p-DVCS, CS, BCA

CERN
<i>COMPASS</i>
p-DVCS CS, BSA, BCA, tTSA, ITSA, DSA



CLAS, HERMES: first observation of DVCS-BH interference in the beam-spin asymmetry (2001)

Hall A: test of scaling for DVCS (2006)



Ongoing and future programs

S. Niccolai, Transversity 2024

JLab12 DVCS

Observable (target)	12-GeV experiments	CFF sensitivity	Status
$\sigma, \Delta\sigma_{\text{beam}}(p)$	Hall A	$\text{Re}\mathcal{H}(p), \text{Im}\mathcal{H}(p)$	Data taken in 2016; Phys. Rev. Lett. 128 (2022)
	CLAS12		Data taken in 2018-2019; CS analysis under review
	Hall C		Experiment just finished
BSA(p) + TCS	CLAS12	$\text{Im}\mathcal{H}(p)$	Data taken in 2018-2019; Phys. Rev. Lett. 130 (2023) Phys. Rev. Lett. 127 (2021)
ITSA(p), IDSA(p)	CLAS12	$\text{Im}\tilde{\mathcal{H}}(p), \text{Im}\mathcal{H}(p), \text{Re}\tilde{\mathcal{H}}(p), \text{Re}\mathcal{H}(p)$	Experiment completed in March 2023
tTSA(p)	CLAS12	$\text{Im}\mathcal{H}(p), \text{Im}\mathcal{E}(p)$	Experiment foreseen for > 2027
BSA(n)	CLAS12	$\text{Im}\mathcal{E}(n)$	Data taken in 2019-2020; BSA paper ready for release
ITSA(n), IDSA(n)	CLAS12	$\text{Im}\mathcal{H}(n), \text{Re}\mathcal{H}(n)$	Experiment completed in March 2023

← first ever TCS

↖ flavor sep. of CFF
↘ Ji's sum rule

combining Hermes & Hall A p DVCS + CLAS12 BSA on p,n DVCS → flavor separation of CFF
+ plans for **DDVCS** and **positron DVCS** Kumericki et al., JHEP 07 (11) 073

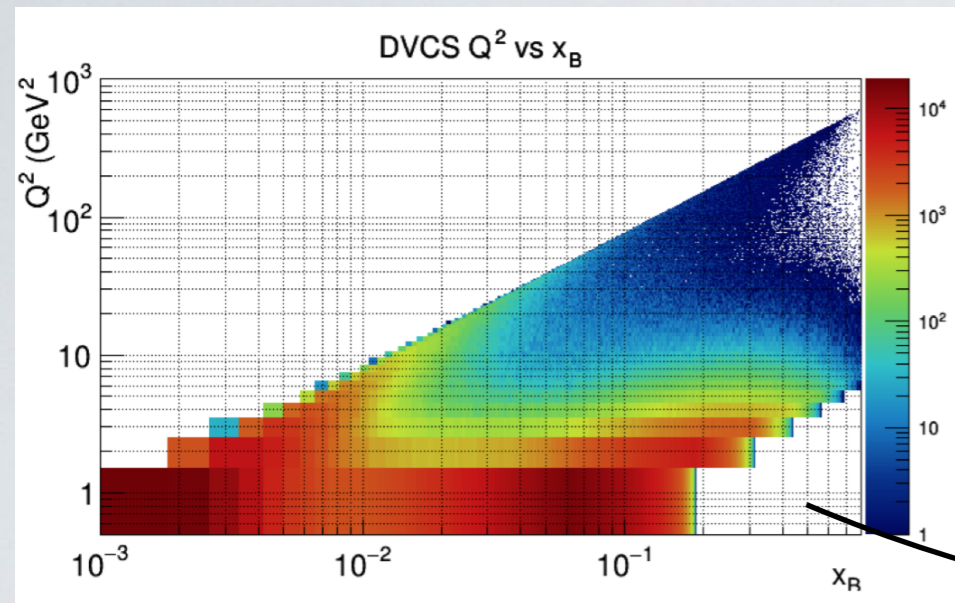
COMPASS DVCS

DVMP on $\pi^0, \rho^0, \omega, \phi, J/\psi$ using 2016,17 data →

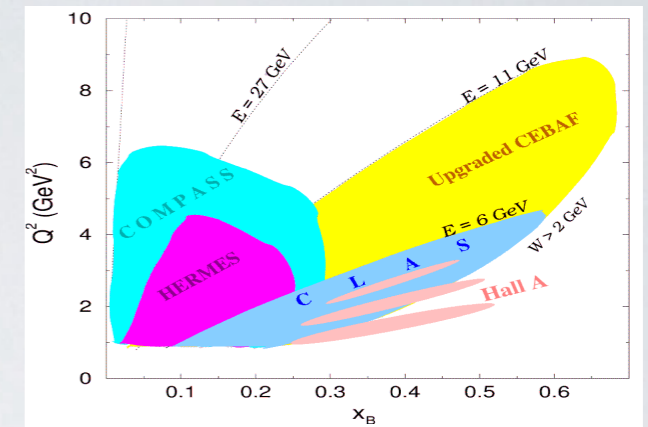
- transversity GPD
- gluon GPD
- flavor decomposition

see N. d'Hose, Transversity 2024

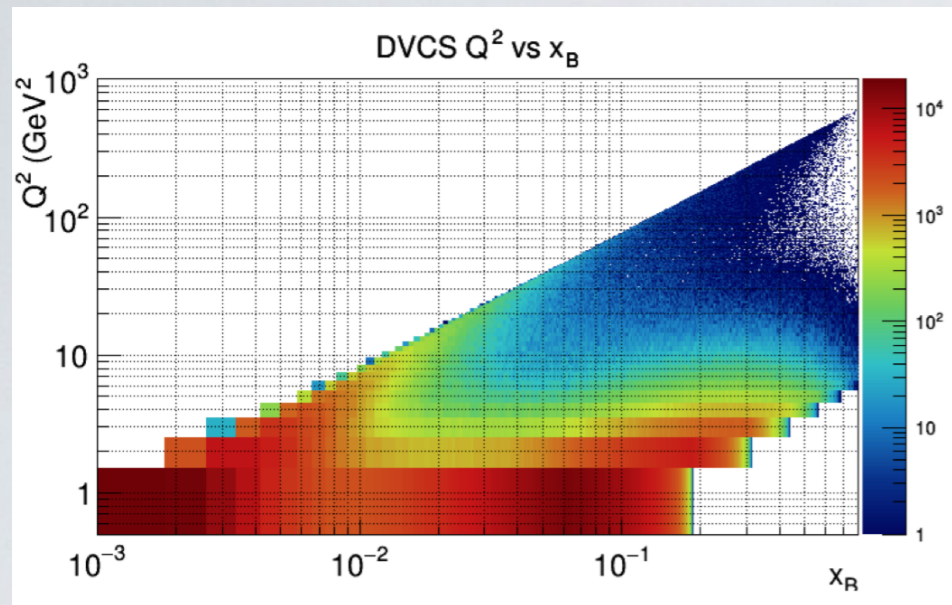
The EIC at low/medium energy: CFF



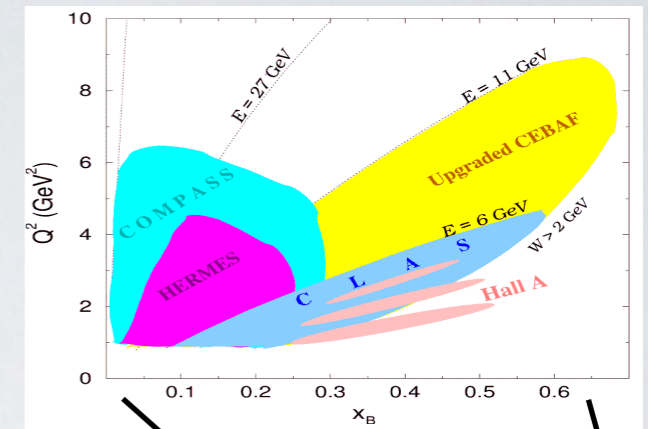
DVCS events / pixel
 $\sqrt{s} = 31$ GeV
assumed integrated
luminosity of 200 fb⁻¹
(Fig.8 paper)



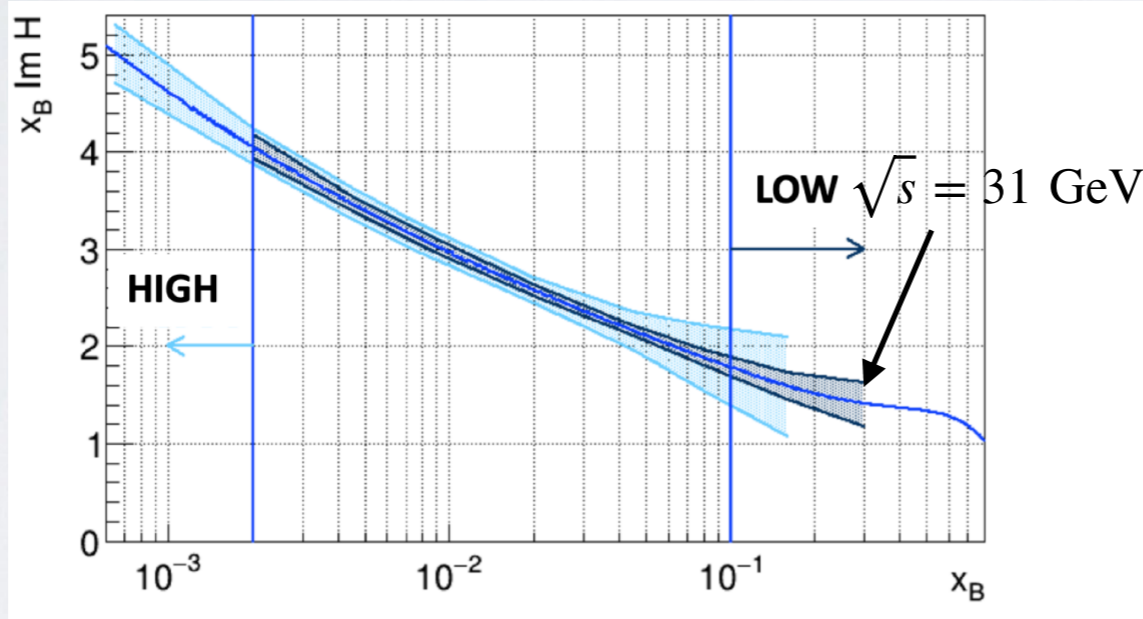
The EIC at low/medium energy: CFF



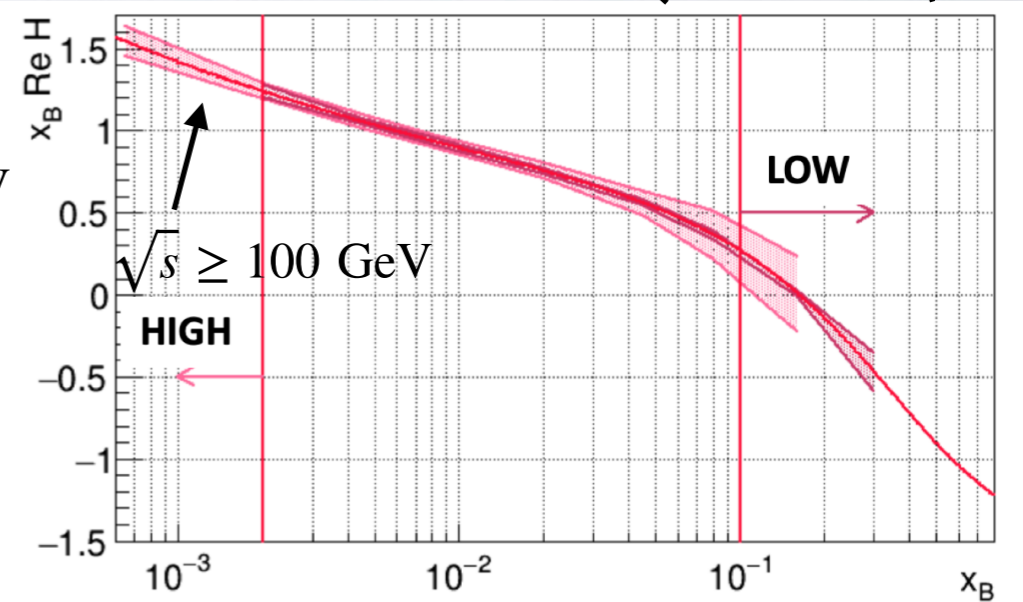
DVCS events / pixel
 $\sqrt{s} = 31 \text{ GeV}$
 assumed integrated
 luminosity of 200 fb^{-1}
 (Fig.8 paper)



$x_B \text{ Im}[\mathcal{H}]$



$x_B \text{ Re}[\mathcal{H}]$

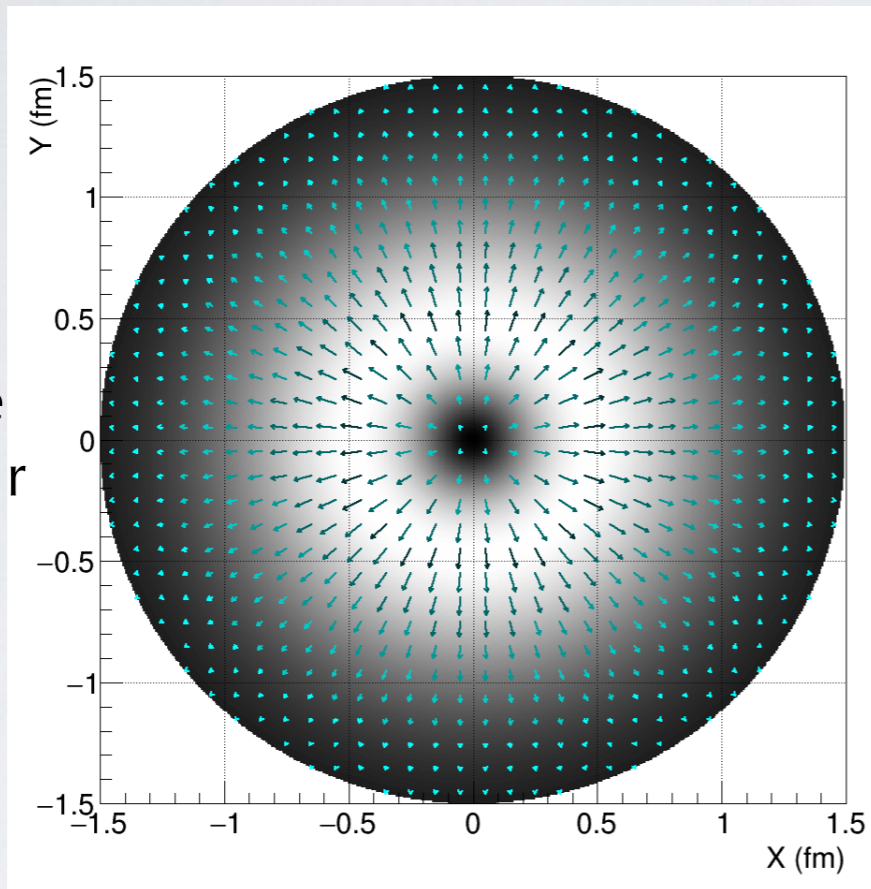


simulated DVCS events at the EIC (Fig.7 of paper)

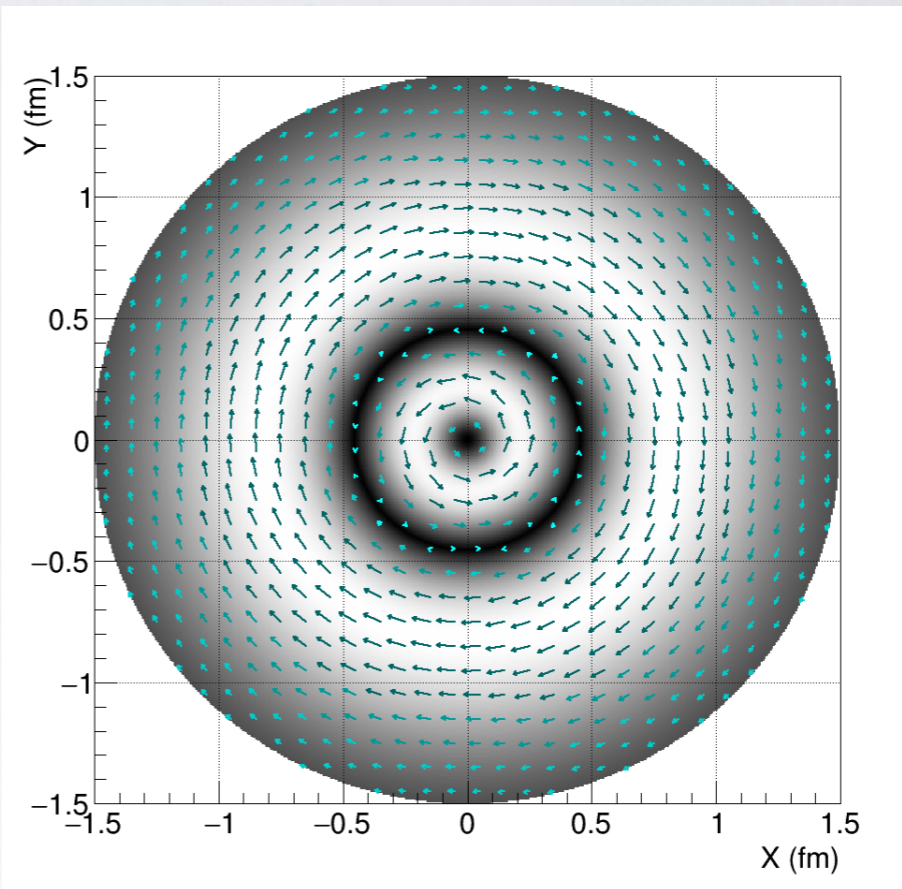
the EIC at low energy can complement
 fixed-target data with higher precision

The EIC at low/medium energy: D-term

radial force



tangential force

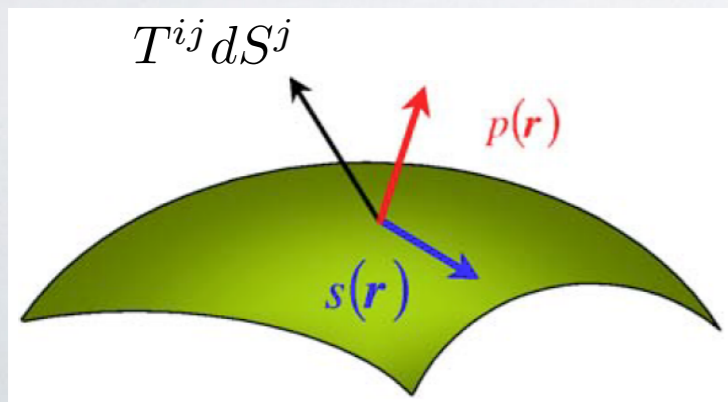


node at
 $r \sim 0.45$ fm
then
changes sign

always positive
fades away with r

(Fig.13 paper)

stress tensor



The EIC at low/medium energy: N mass

QCD EMT

$$\langle P' | T_{\mu\nu}^{q,g} | P \rangle = \bar{u}(P') \left[M^{q,g}(t) \frac{P_\mu P_\nu}{M_N} + J^{q,g}(t) \frac{i(P_\mu \sigma_{\nu\rho} + P_\nu \sigma_{\mu\rho}) \Delta^\rho}{2M_N} + D^{q,g}(t) \frac{\Delta_\mu \Delta_\nu - g_{\mu\nu} \Delta^2}{5M_N} + \bar{c}_{q,g}(t) g_{\mu\nu} \right] u(P)$$

N mass

$$M_N \rightarrow \langle P | T_{00}^q + T_{00}^g | P \rangle =$$

The EIC at low/medium energy: N mass

QCD EMT

$$\langle P' | T_{\mu\nu}^{q,g} | P \rangle = \bar{u}(P') \left[M^{q,g}(t) \frac{P_\mu P_\nu}{M_N} + J^{q,g}(t) \frac{i(P_\mu \sigma_{\nu\rho} + P_\nu \sigma_{\mu\rho}) \Delta^\rho}{2M_N} + D^{q,g}(t) \frac{\Delta_\mu \Delta_\nu - g_{\mu\nu} \Delta^2}{5M_N} + \bar{c}_{q,g}(t) g_{\mu\nu} \right] u(P)$$

N mass

$$M_N \rightarrow \langle P | T_{00}^q + T_{00}^g | P \rangle = \mathbf{E}_q + \mathbf{E}_g$$

relativistic motion
of quarks and gluons
(~70% ?)

The EIC at low/medium energy: N mass

QCD EMT

$$\langle P' | T_{\mu\nu}^{q,g} | P \rangle = \bar{u}(P') \left[M^{q,g}(t) \frac{P_\mu P_\nu}{M_N} + J^{q,g}(t) \frac{i(P_\mu \sigma_{\nu\rho} + P_\nu \sigma_{\mu\rho}) \Delta^\rho}{2M_N} + D^{q,g}(t) \frac{\Delta_\mu \Delta_\nu - g_{\mu\nu} \Delta^2}{5M_N} + \bar{c}_{q,g}(t) g_{\mu\nu} \right] u(P)$$

N mass

$$M_N \rightarrow \langle P | T_{00}^q + T_{00}^g | P \rangle = \mathbf{E}_q + \mathbf{E}_g + \bar{c}_q(0) \left(= \langle \bar{\psi} m \psi \rangle \right) + \bar{c}_g(0) \left(= \left\langle \frac{\beta(g)}{2g} F^{\mu\nu} F_{\mu\nu} + \gamma_m \bar{\psi} m \psi \right\rangle \right)$$

relativistic motion
of quarks and gluons
(~70% ?)
quark condensate
σ-term from πN scatt.
(~9%?)
trace anomaly M_a
?

The EIC at low/medium energy: N mass

QCD EMT

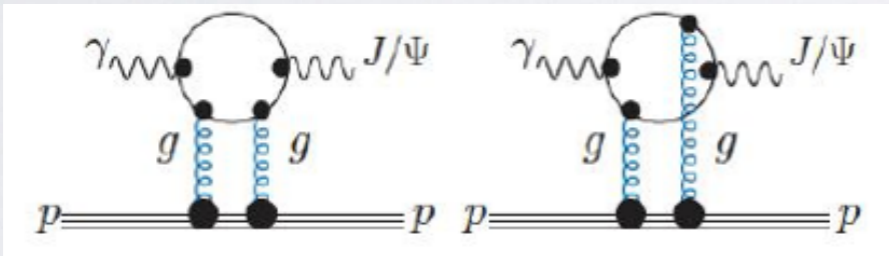
$$\langle P' | T_{\mu\nu}^{q,g} | P \rangle = \bar{u}(P') \left[M^{q,g}(t) \frac{P_\mu P_\nu}{M_N} + J^{q,g}(t) \frac{i(P_\mu \sigma_{\nu\rho} + P_\nu \sigma_{\mu\rho}) \Delta^\rho}{2M_N} + D^{q,g}(t) \frac{\Delta_\mu \Delta_\nu - g_{\mu\nu} \Delta^2}{5M_N} + \bar{c}_{q,g}(t) g_{\mu\nu} \right] u(P)$$

N mass

$$M_N \rightarrow \langle P | T_{00}^q + T_{00}^g | P \rangle = \mathbf{E}_q + \mathbf{E}_g + \bar{c}_q(0) \left(= \langle \bar{\psi} m \psi \rangle \right) + \bar{c}_g(0) \left(= \left\langle \frac{\beta(g)}{2g} F^{\mu\nu} F_{\mu\nu} + \gamma_m \bar{\psi} m \psi \right\rangle \right)$$

relativistic motion
of quarks and gluons
(~70% ?)
quark condensate
σ-term from πN scatt.
(~9%?)
trace anomaly M_a
?

threshold γ - and e-production of J/ψ or Υ



$$\frac{d\sigma}{dt} \sim |\mathcal{M}_{\gamma p \rightarrow J/\psi}(t)|^2 \sim |\langle P' | T_{\mu}^{\mu g} | P \rangle|^2 \xrightarrow{t \rightarrow 0} M_a$$

The EIC at low/medium energy: N mass

QCD EMT

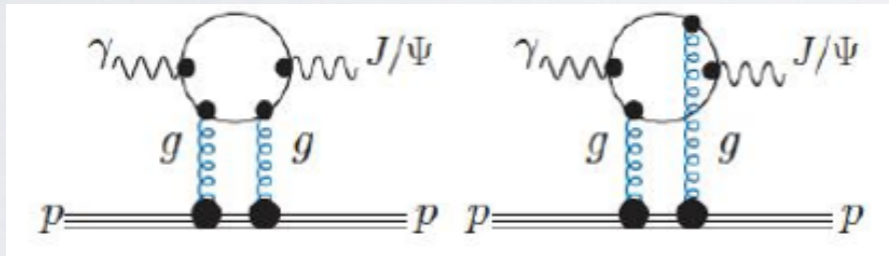
$$\langle P' | T_{\mu\nu}^{q,g} | P \rangle = \bar{u}(P') \left[M^{q,g}(t) \frac{P_\mu P_\nu}{M_N} + J^{q,g}(t) \frac{i(P_\mu \sigma_{\nu\rho} + P_\nu \sigma_{\mu\rho}) \Delta^\rho}{2M_N} + D^{q,g}(t) \frac{\Delta_\mu \Delta_\nu - g_{\mu\nu} \Delta^2}{5M_N} + \bar{c}_{q,g}(t) g_{\mu\nu} \right] u(P)$$

N mass

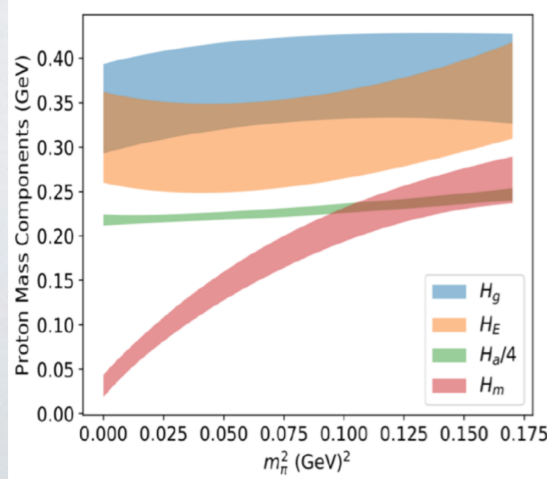
$$M_N \rightarrow \langle P | T_{00}^q + T_{00}^g | P \rangle = \mathbf{E}_q + \mathbf{E}_g + \bar{c}_q(0) \left(= \langle \bar{\psi} m \psi \rangle \right) + \bar{c}_g(0) \left(= \left\langle \frac{\beta(g)}{2g} F^{\mu\nu} F_{\mu\nu} + \gamma_m \bar{\psi} m \psi \right\rangle \right)$$

relativistic motion of quarks and gluons (~70% ?)
quark condensate σ -term from πN scatt. (~9%?)
trace anomaly M_a ?

threshold γ - and e-production of J/ψ or Υ



$$\frac{d\sigma}{dt} \sim |\mathcal{M}_{\gamma p \rightarrow J/\psi}(t)|^2 \sim |\langle P' | T_{\mu}^{\mu g} | P \rangle|^2 \xrightarrow{t \rightarrow 0} M_a$$



Alexandrou et al.,
P.R.L. **119** (17) 142002

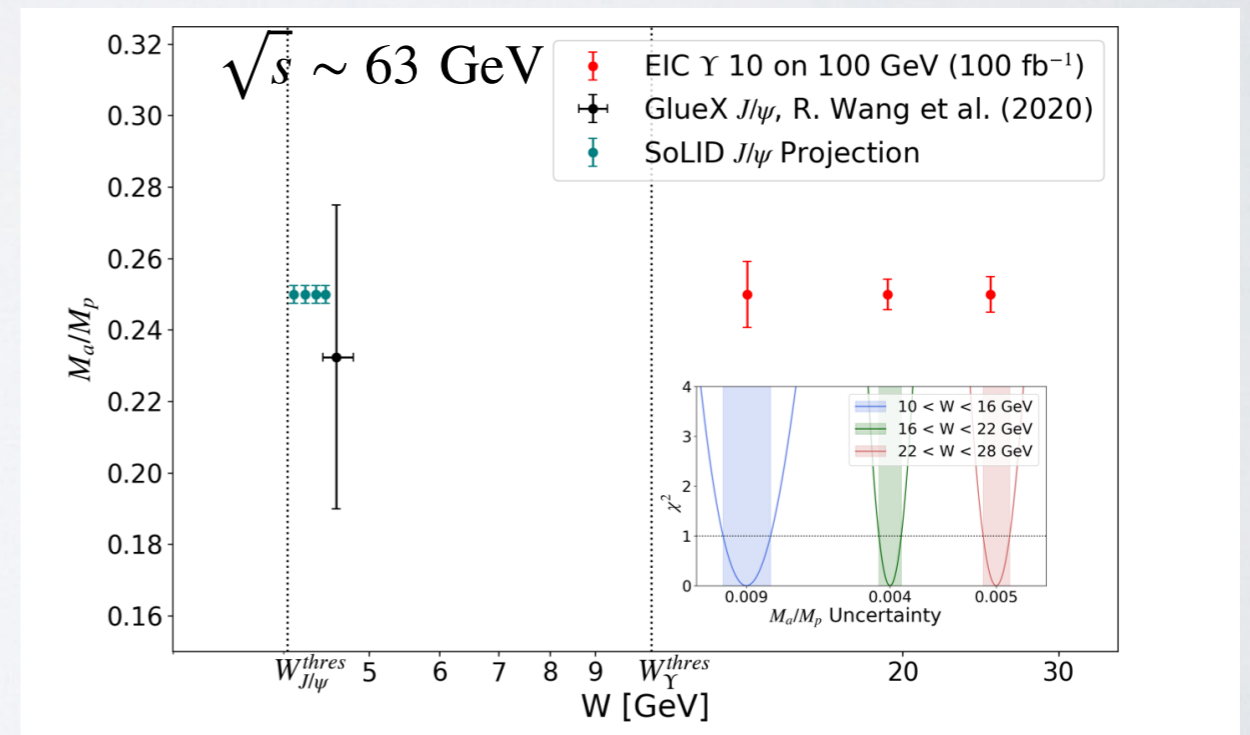
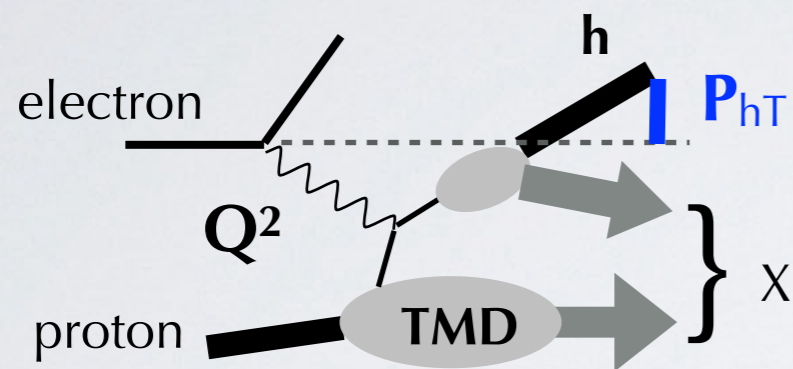


Figure 7.26: Projection of the trace anomaly contribution to the proton mass (M_a/M_p) with Υ photoproduction on the proton at the EIC in 10×100 GeV electron/proton beam-energy

Semi-inclusive processes

IV. Accessing the Momentum Dependent Structure of the nucleon in Semi-Inclusive Deep Inelastic Scattering

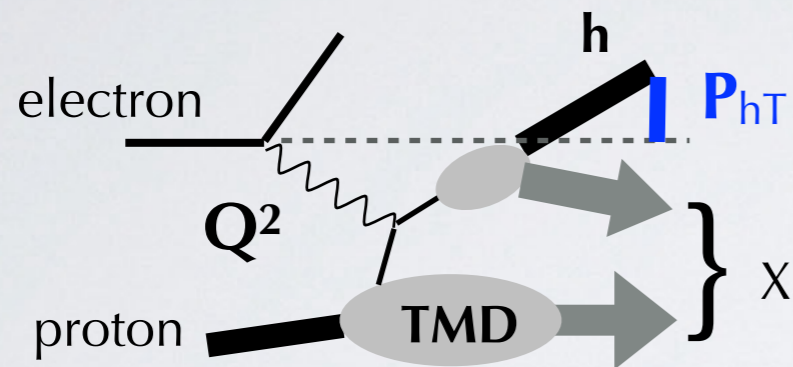


factorization if $\mathbf{q}_T = \mathbf{P}_{hT}/z \ll Q$
 \mathbf{P}_{hT} “feels” intrinsic \mathbf{k}_T of confined motion

Ji, Yuan, Ma, P.R. **D71** (05)
Rogers & Aybat, P.R. **D83** (11)
Collins, “Foundations of Perturbative QCD” (11)
Echevarria, Idilbi, Scimemi, JHEP **1207** (12)

Semi-inclusive processes

IV. Accessing the Momentum Dependent Structure of the nucleon in Semi-Inclusive Deep Inelastic Scattering



factorization if $\mathbf{q}_T = \mathbf{P}_{hT}/z \ll Q$
 \mathbf{P}_{hT} "feels" intrinsic \mathbf{k}_T of confined motion

Ji, Yuan, Ma, P.R. **D71** (05)
 Rogers & Aybat, P.R. **D83** (11)
 Collins, "Foundations of Perturbative QCD" (11)
 Echevarria, Idilbi, Scimemi, JHEP **1207** (12)

affinity = probability to fulfill fact. th.

Boglione et al., JHEP **04** (22) 084

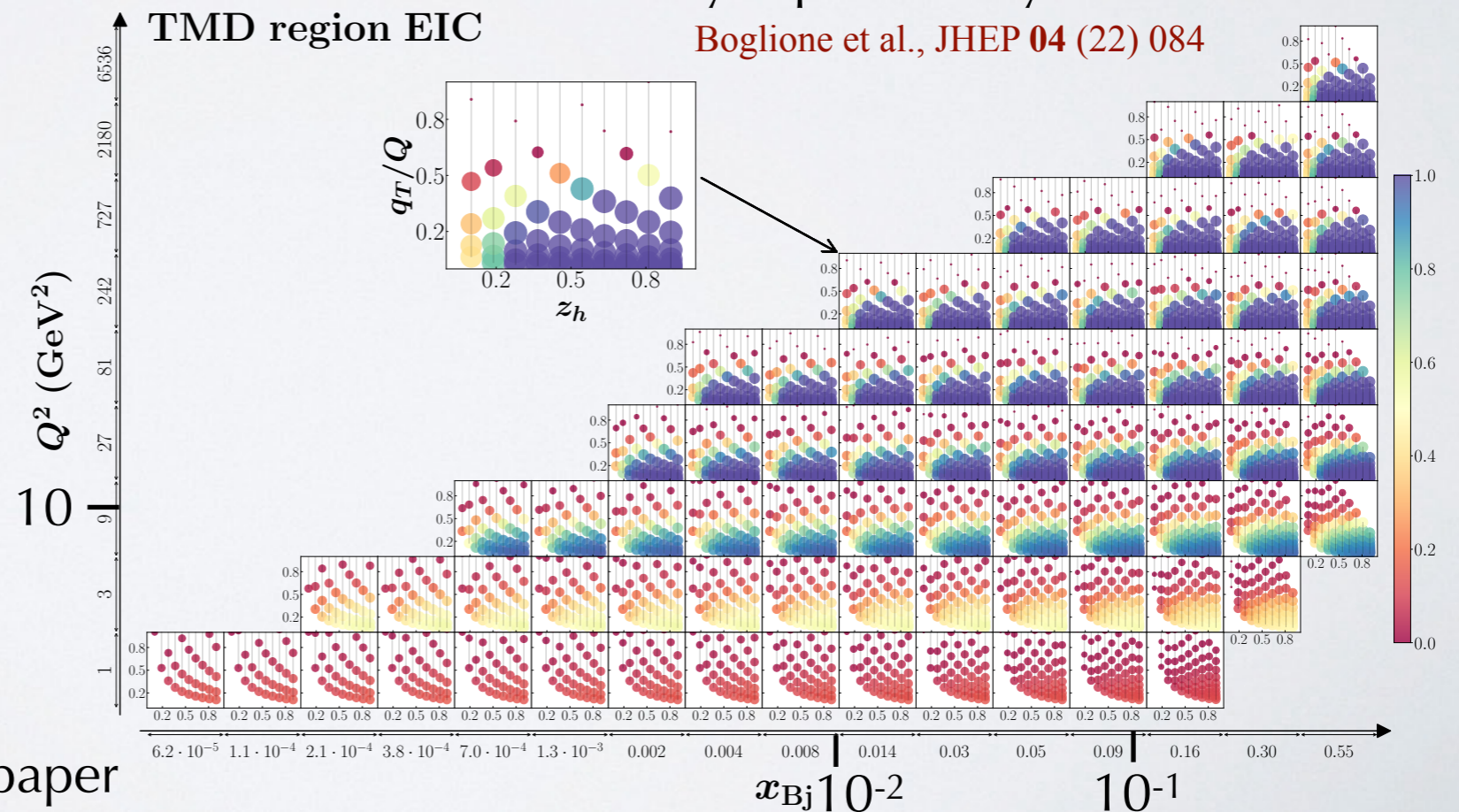
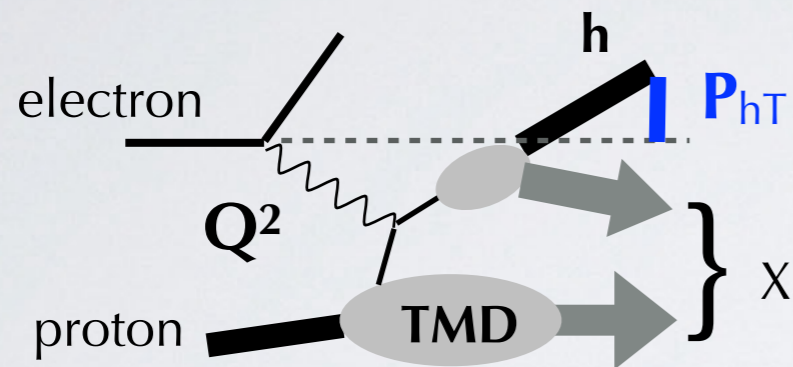


Fig.23 of paper

Semi-inclusive processes

IV. Accessing the Momentum Dependent Structure of the nucleon in Semi-Inclusive Deep Inelastic Scattering

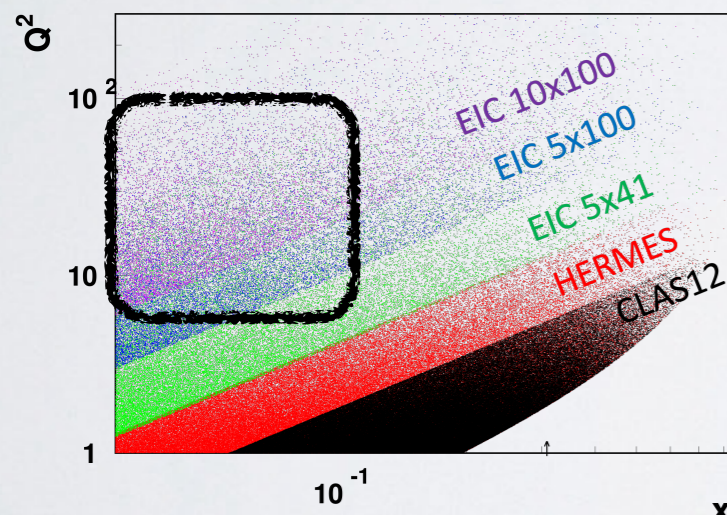


factorization if $\mathbf{q}_T = \mathbf{P}_{hT}/z \ll Q$
 \mathbf{P}_{hT} "feels" intrinsic \mathbf{k}_T of confined motion

Ji, Yuan, Ma, P.R. **D71** (05)
 Rogers & Aybat, P.R. **D83** (11)
 Collins, "Foundations of Perturbative QCD" (11)
 Echevarria, Idilbi, Scimemi, JHEP **1207** (12)

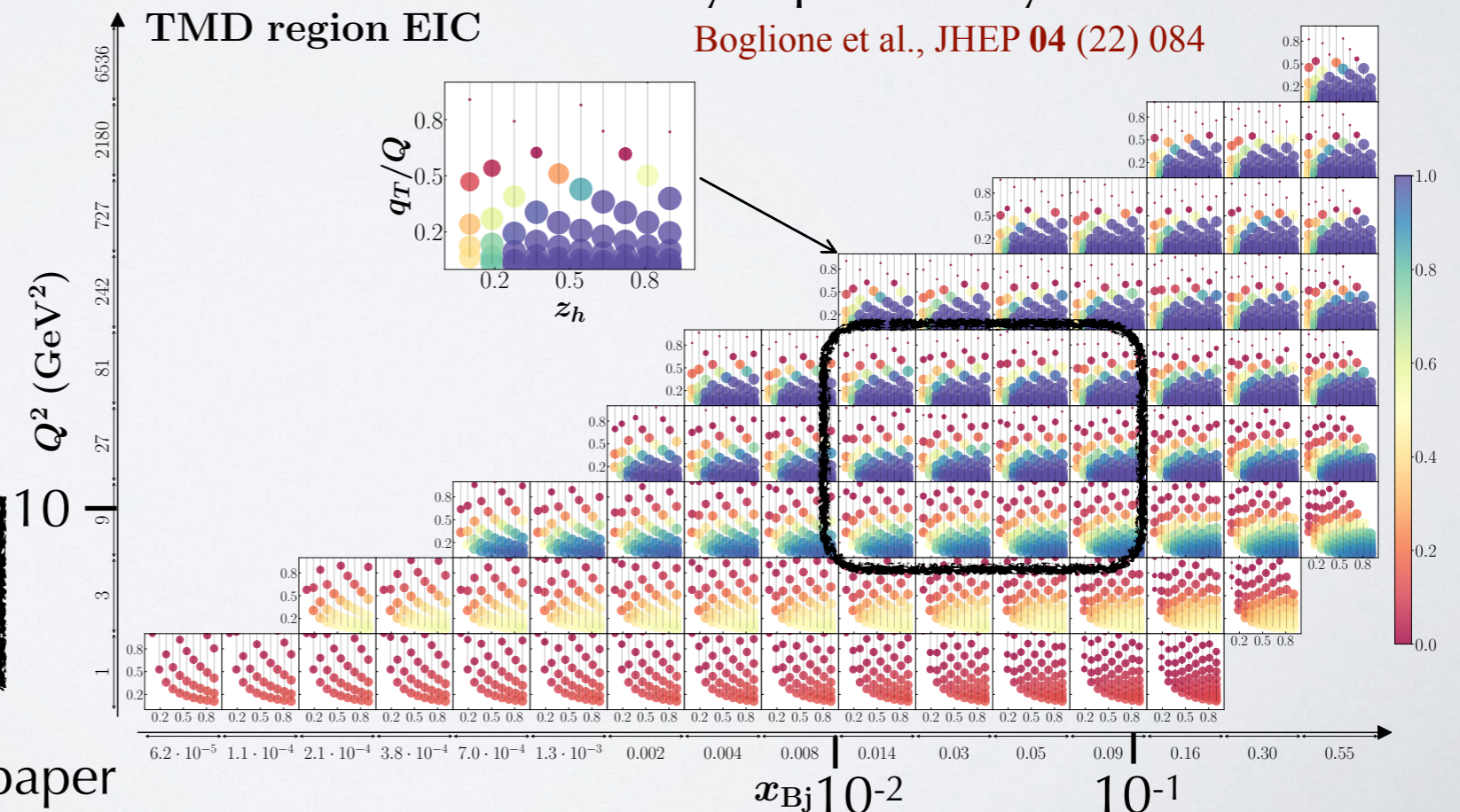
affinity = probability of fulfill fact. th.

Boglionne et al., JHEP **04** (22) 084



EIC low/medium energy well into TMD factorization region

Fig.23 of paper



SIDIS cross section

$$\begin{aligned}
 \frac{d\sigma}{dx dy dz dp_T^2 d\phi_h d\phi_S} = & \quad \text{twist-2 } A_{XX} \\
 & \quad \text{twist-3 } A_{XX} \\
 & \left[\frac{\alpha}{xyQ^2} \frac{y^2}{2(1-\varepsilon)} \left(1 + \frac{\gamma^2}{2x} \right) \right] (F_{UU,T} + \varepsilon F_{UU,L}) \quad \text{target pol.} \\
 & \times \left\{ \begin{array}{l}
 \begin{array}{l}
 1 + \sqrt{2\varepsilon(1+\varepsilon)} A_{UU}^{\cos\phi_h} \cos\phi_h + \varepsilon A_{UU}^{\cos 2\phi_h} \cos 2\phi_h \\
 + \lambda \sqrt{2\varepsilon(1-\varepsilon)} A_{LU}^{\sin\phi_h} \sin\phi_h
 \end{array} \quad \text{U} \\
 \begin{array}{l}
 + S_L \left[\sqrt{2\varepsilon(1+\varepsilon)} A_{UL}^{\sin\phi_h} \sin\phi_h + \varepsilon A_{UL}^{\sin 2\phi_h} \sin 2\phi_h \right] \\
 + S_L \lambda \left[\sqrt{1-\varepsilon^2} A_{LL} + \sqrt{2\varepsilon(1-\varepsilon)} A_{LL}^{\cos\phi_h} \cos\phi_h \right]
 \end{array} \quad \text{L} \\
 \begin{array}{l}
 + S_T \left[\begin{array}{l}
 A_{UT}^{\sin(\phi_h-\phi_S)} \sin(\phi_h-\phi_S) \\
 + \varepsilon A_{UT}^{\sin(\phi_h+\phi_S)} \sin(\phi_h+\phi_S) \\
 + \varepsilon A_{UT}^{\sin(3\phi_h-\phi_S)} \sin(3\phi_h-\phi_S) \\
 + \sqrt{2\varepsilon(1+\varepsilon)} A_{UT}^{\sin\phi_S} \sin\phi_S \\
 + \sqrt{2\varepsilon(1+\varepsilon)} A_{UT}^{\sin(2\phi_h-\phi_S)} \sin(2\phi_h-\phi_S)
 \end{array} \right] \\
 + S_T \lambda \left[\begin{array}{l}
 \sqrt{(1-\varepsilon^2)} A_{LT}^{\cos(\phi_h-\phi_S)} \cos(\phi_h-\phi_S) \\
 + \sqrt{2\varepsilon(1-\varepsilon)} A_{LT}^{\cos\phi_S} \cos\phi_S \\
 + \sqrt{2\varepsilon(1-\varepsilon)} A_{LT}^{\cos(2\phi_h-\phi_S)} \cos(2\phi_h-\phi_S)
 \end{array} \right]
 \end{array} \quad \text{T}
 \end{array} \right.
 \end{aligned}$$

SIDIS cross section

$$\frac{d\sigma}{dx dy dz dp_T^2 d\phi_h d\phi_S} = \left[\frac{\alpha}{xyQ^2} \frac{y^2}{2(1-\varepsilon)} \left(1 + \frac{\gamma^2}{2x} \right) \right] (F_{UU,T} + \varepsilon F_{UU,L})$$

twist-2 A_{XX}
twist-3 A_{XX}

target pol.

$$\begin{aligned} & \left[1 + \sqrt{2\varepsilon(1+\varepsilon)} A_{UU}^{\cos\phi_h} \cos\phi_h + \varepsilon A_{UU}^{\cos 2\phi_h} \cos 2\phi_h \right. \\ & \quad \left. + \lambda \sqrt{2\varepsilon(1-\varepsilon)} A_{LU}^{\sin\phi_h} \sin\phi_h \right] \\ & + S_L \left[\sqrt{2\varepsilon(1+\varepsilon)} A_{UL}^{\sin\phi_h} \sin\phi_h + \varepsilon A_{UL}^{\sin 2\phi_h} \sin 2\phi_h \right] \\ & + S_L \lambda \left[\sqrt{1-\varepsilon^2} A_{LL} + \sqrt{2\varepsilon(1-\varepsilon)} A_{LL}^{\cos\phi_h} \cos\phi_h \right] \\ & \times \left\{ \begin{aligned} & A_{UT}^{\sin(\phi_h-\phi_S)} \sin(\phi_h-\phi_S) \\ & + \varepsilon A_{UT}^{\sin(\phi_h+\phi_S)} \sin(\phi_h+\phi_S) \\ & + \varepsilon A_{UT}^{\sin(3\phi_h-\phi_S)} \sin(3\phi_h-\phi_S) \\ & + \sqrt{2\varepsilon(1+\varepsilon)} A_{UT}^{\sin\phi_S} \sin\phi_S \\ & + \sqrt{2\varepsilon(1+\varepsilon)} A_{UT}^{\sin(2\phi_h-\phi_S)} \sin(2\phi_h-\phi_S) \\ & + \sqrt{(1-\varepsilon^2)} A_{LT}^{\cos(\phi_h-\phi_S)} \cos(\phi_h-\phi_S) \\ & + S_T \lambda \left[\sqrt{2\varepsilon(1-\varepsilon)} A_{LT}^{\cos\phi_S} \cos\phi_S \right. \\ & \quad \left. + \sqrt{2\varepsilon(1-\varepsilon)} A_{LT}^{\cos(2\phi_h-\phi_S)} \cos(2\phi_h-\phi_S) \right] \end{aligned} \right\} \end{aligned}$$

relative statistical uncertainty

$$\frac{\text{depolar. fact. } (y, \varepsilon)}{[N. \text{ counts } (x, Q^2)]^{1/2}}$$

$$\sqrt{s} \sim 30 \text{ GeV}$$

U

L

T

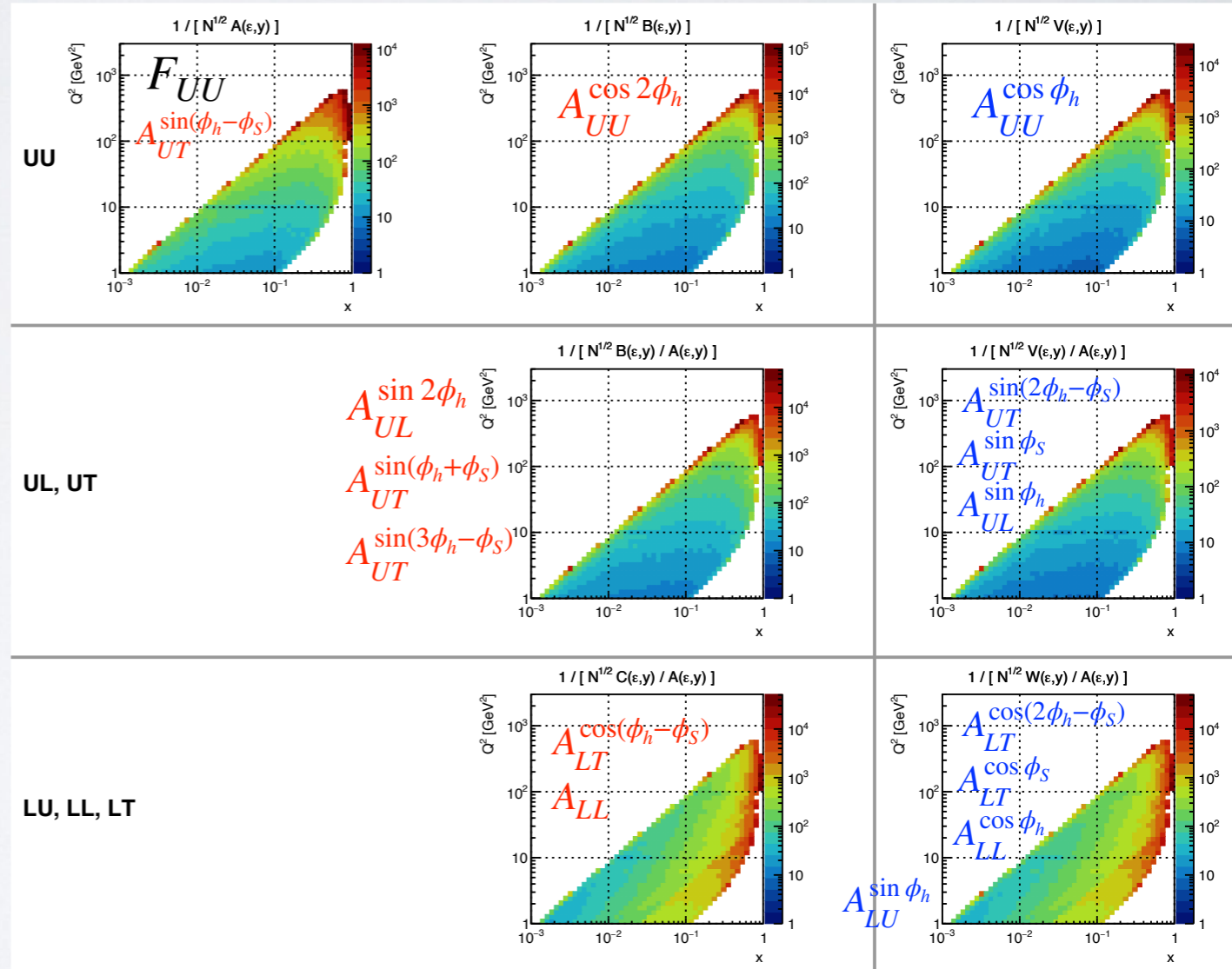


Fig.16 of the paper

SIDIS cross section

$$\frac{d\sigma}{dx dy dz dp_T^2 d\phi_h d\phi_S} = \left[\frac{\alpha}{xyQ^2} \frac{y^2}{2(1-\varepsilon)} \left(1 + \frac{\gamma^2}{2x} \right) \right] (F_{UU,T} + \varepsilon F_{UU,L})$$

twist-2 A_{XX}
twist-3 A_{XX}

target pol.

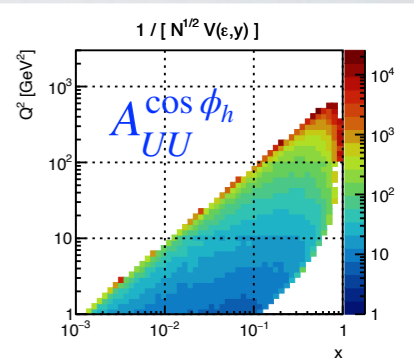
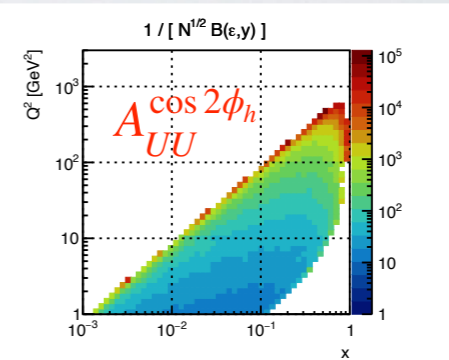
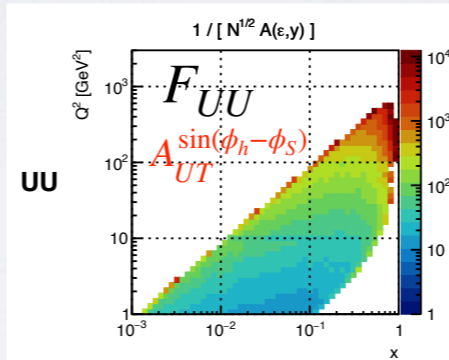
relative statistical uncertainty

$$\frac{\text{depolar. fact. } (y, \varepsilon)}{[\text{N. counts } (x, Q^2)]^{1/2}}$$

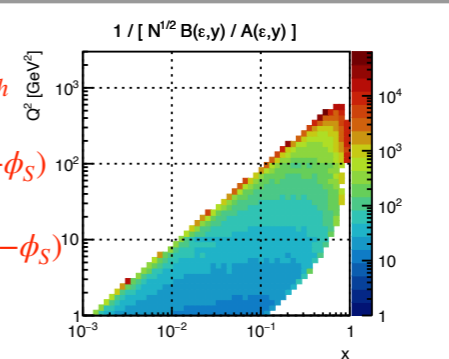
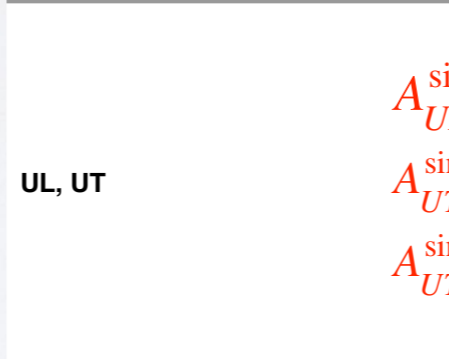
$$\sqrt{s} \sim 30 \text{ GeV}$$

$$\begin{aligned} & \left\{ \begin{aligned} & 1 + \sqrt{2\varepsilon(1+\varepsilon)} A_{UU}^{\cos\phi_h} \cos\phi_h + \varepsilon A_{UU}^{\cos 2\phi_h} \cos 2\phi_h \\ & + \lambda \sqrt{2\varepsilon(1-\varepsilon)} A_{LU}^{\sin\phi_h} \sin\phi_h \\ & + S_L \left[\sqrt{2\varepsilon(1+\varepsilon)} A_{UL}^{\sin\phi_h} \sin\phi_h + \varepsilon A_{UL}^{\sin 2\phi_h} \sin 2\phi_h \right] \\ & + S_L \lambda \left[\sqrt{1-\varepsilon^2} A_{LL} + \sqrt{2\varepsilon(1-\varepsilon)} A_{LL}^{\cos\phi_h} \cos\phi_h \right] \end{aligned} \right. \\ & \times \left\{ \begin{aligned} & A_{UT}^{\sin(\phi_h - \phi_S)} \sin(\phi_h - \phi_S) \\ & + \varepsilon A_{UT}^{\sin(\phi_h + \phi_S)} \sin(\phi_h + \phi_S) \\ & + S_T \left[\varepsilon A_{UT}^{\sin(3\phi_h - \phi_S)} \sin(3\phi_h - \phi_S) \right. \\ & \quad + \sqrt{2\varepsilon(1+\varepsilon)} A_{UT}^{\sin\phi_S} \sin\phi_S \\ & \quad \left. + \sqrt{2\varepsilon(1+\varepsilon)} A_{UT}^{\sin(2\phi_h - \phi_S)} \sin(2\phi_h - \phi_S) \right] \\ & + S_T \lambda \left[\sqrt{(1-\varepsilon^2)} A_{LT}^{\cos(\phi_h - \phi_S)} \cos(\phi_h - \phi_S) \right. \\ & \quad \left. + \sqrt{2\varepsilon(1-\varepsilon)} A_{LT}^{\cos\phi_S} \cos\phi_S \right] \end{aligned} \right. \end{aligned}$$

U

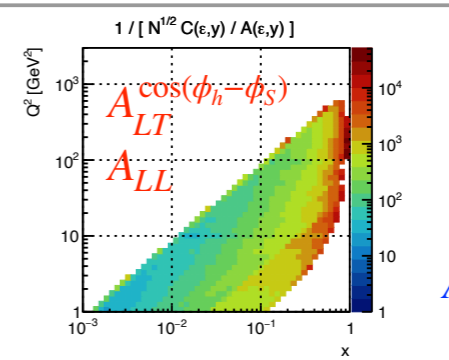


L



UL, UT

T



LU, LL, LT

For EIC at low/medium energy very low statistical uncertainties for UU, UL, UT

Fig.16 of the paper

EIC impact on unpol. TMD

unpolarized cross section $e p \rightarrow e' + \pi^+ + X$

Adam et al. (ATHENA Coll.), JINST 17 (22) P10019

th. uncertainty from PV17 fit
(global fit of SIDIS + Drell-Yan)

Bacchetta et al., JHEP 06 (17) 081

ATHENA projected errors
(2% pt-to-pt + 3% scale systematic error)

In each (x, Q^2) , kinematics with largest impact is shown

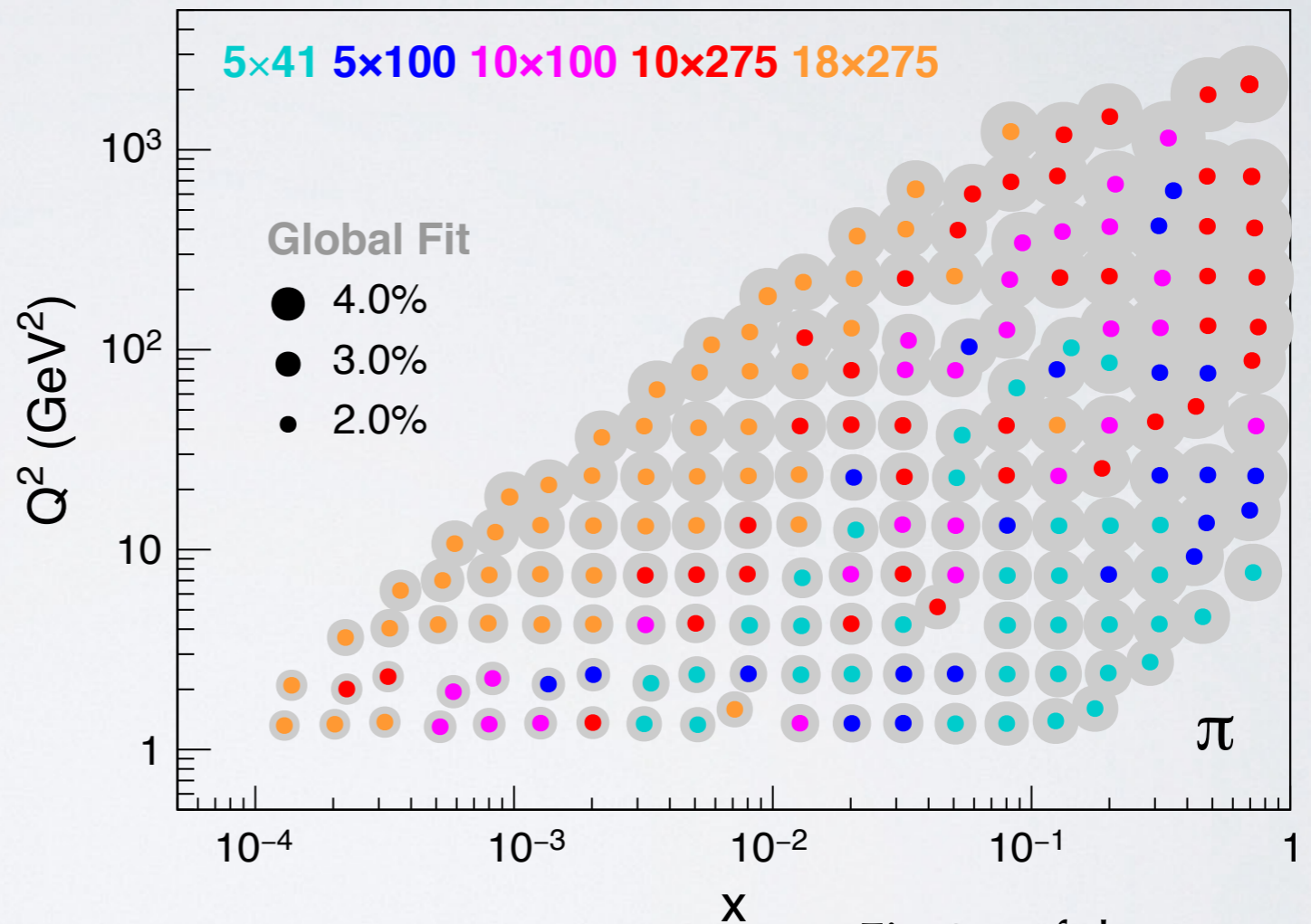


Fig.24 of the paper

EIC impact on unpol. TMD

unpolarized cross section $e p \rightarrow e' + \pi^+ + X$

Adam et al. (ATHENA Coll.), JINST 17 (22) P10019

th. uncertainty from PV17 fit
(global fit of SIDIS + Drell-Yan)

Bacchetta et al., JHEP 06 (17) 081

ATHENA projected errors
(2% pt-to-pt + 3% scale systematic error)

In each (x, Q^2) , kinematics with largest impact is shown

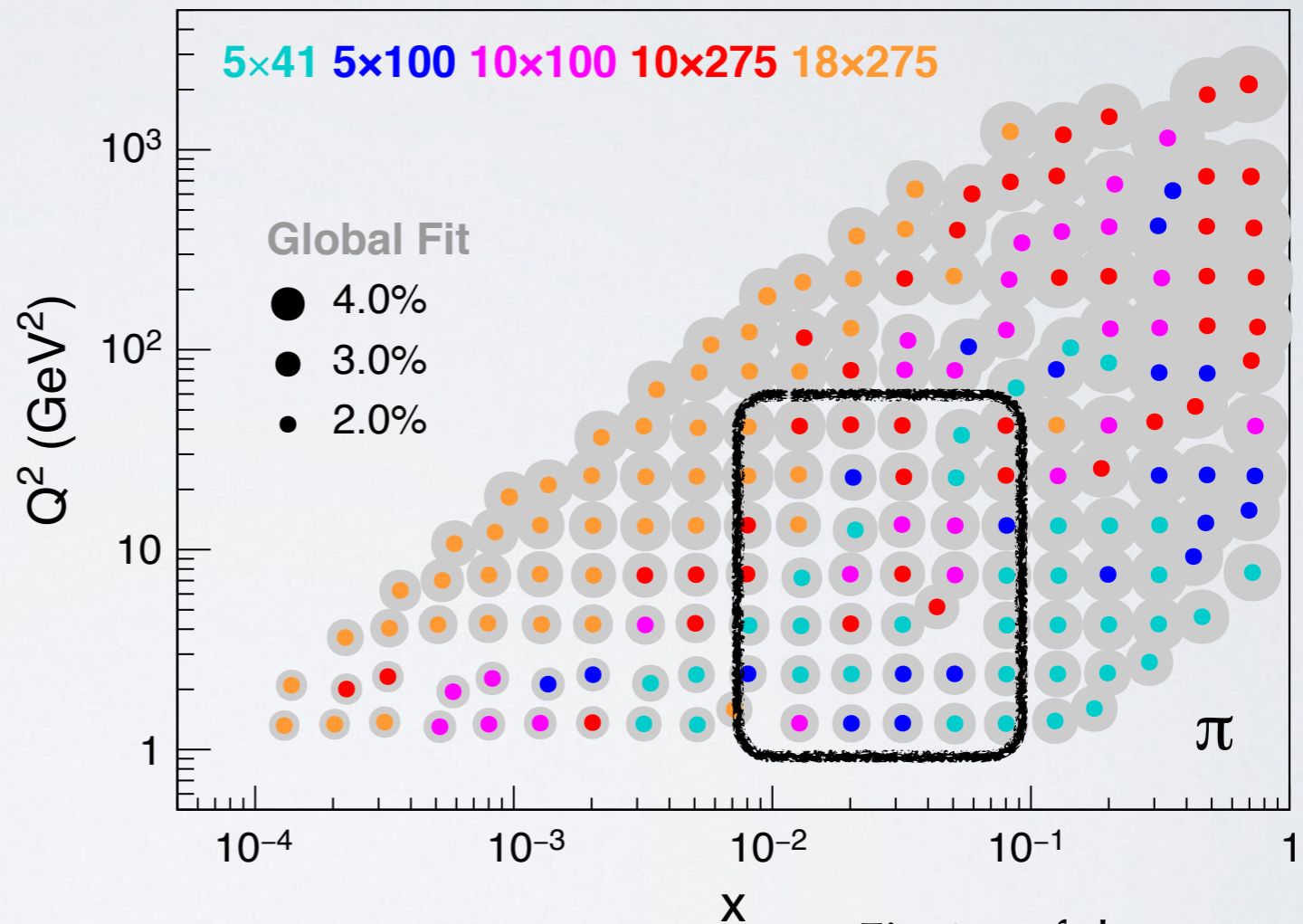
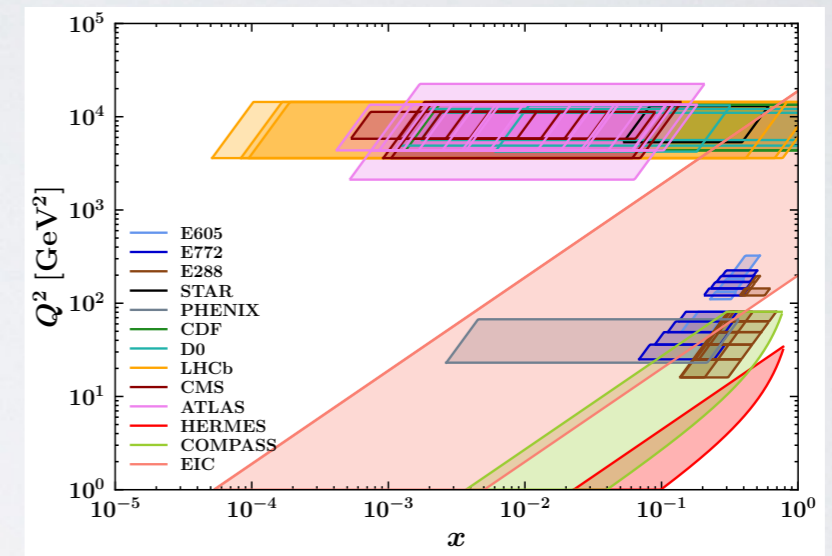
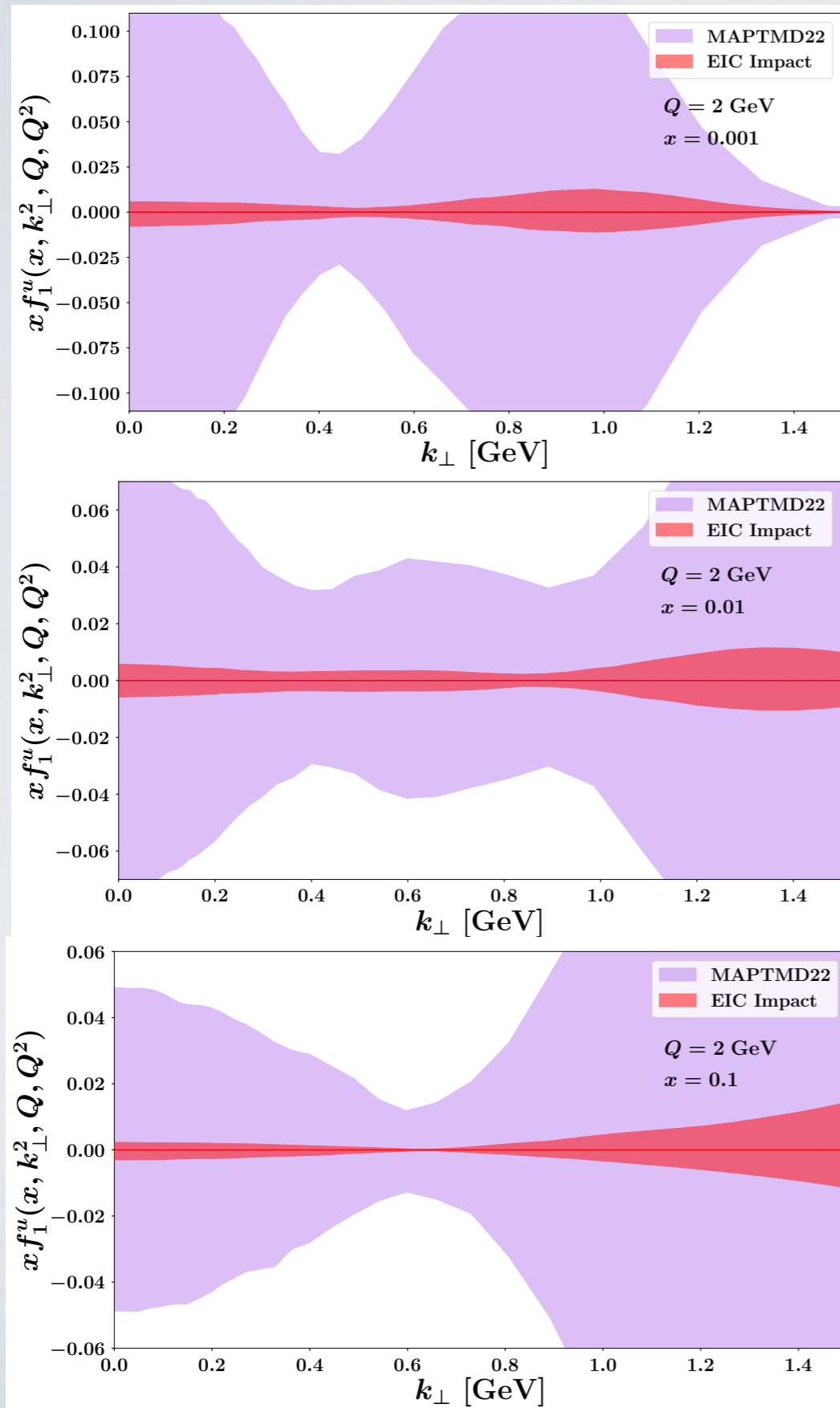


Fig.24 of the paper

major impact from **low/medium** energy configurations

EIC impact on unpol. TMD

MAPTMD22 global fit of
2031 SIDIS + Drell-Yan data
Bacchetta et al. (MAP Coll.), JHEP 10 (22) 127



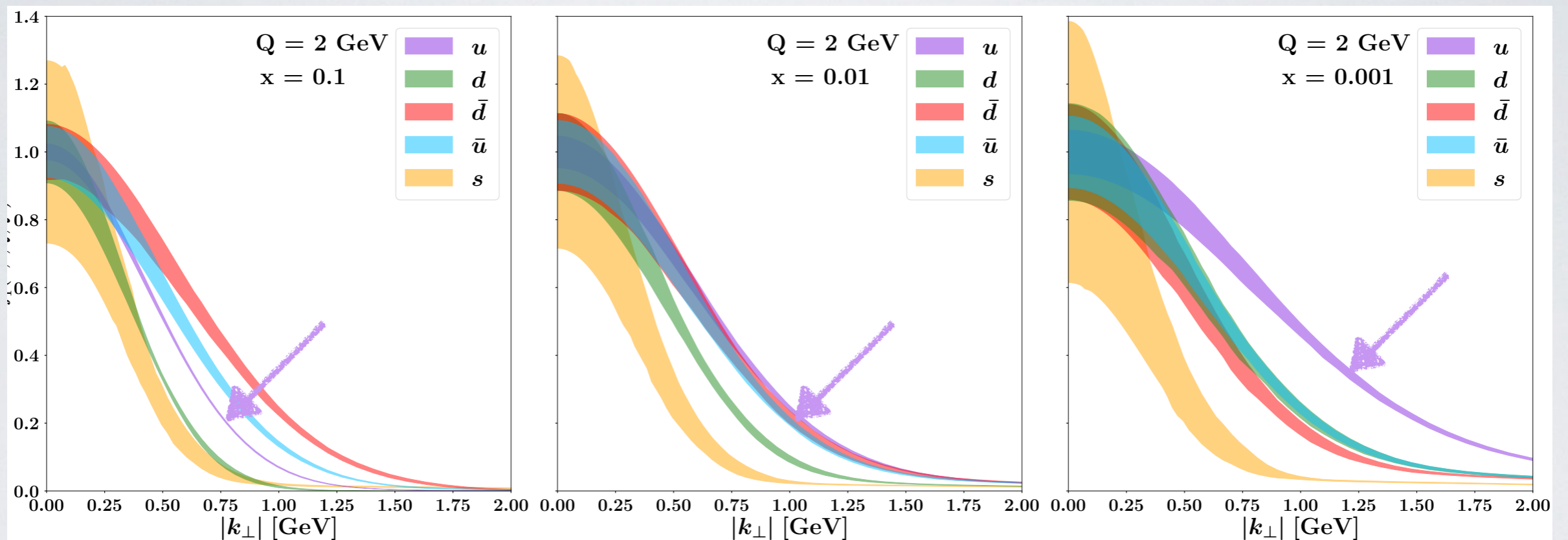
EIC impact at $\sqrt{s} \sim 63$ GeV
already important at $x=0.1$

EIC impact on unpol. TMD

MAPTMD24 global fit of 2031 SIDIS + Drell-Yan data
including flavor dependence of k_T -distribution

Bacchetta et al. (MAP Coll.), arXiv:2405.13833

$$\frac{f_1(x, k_T; Q)}{f_1(x, 0; Q)}$$



- very different k_T behavior
- it changes with x

th. error band =
68% of all replicas

EIC impact on Sivers TMD

TSSA $e p \uparrow \rightarrow e' + \pi^+ + X$

Adam et al. (ATHENA Coll.), JINST 17 (22) P10019

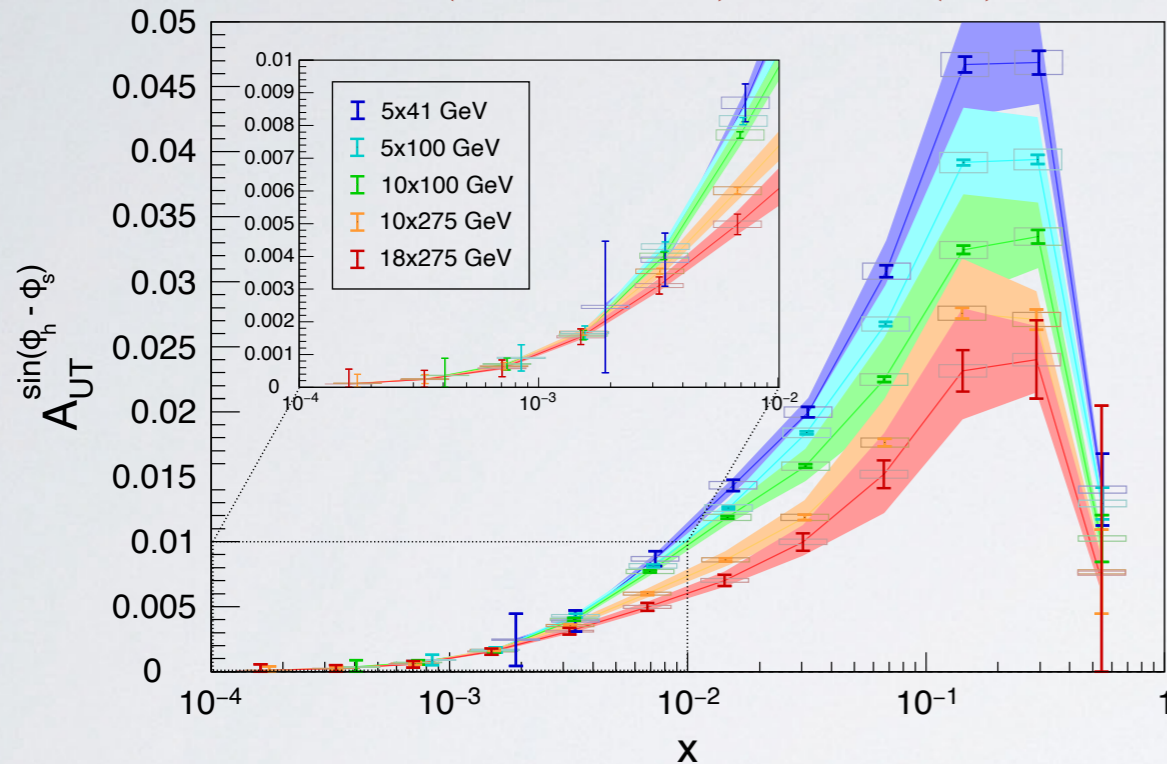


Fig.18 of the paper

Sivers TMD from

Bacchetta et al., P.L. B827 (22) 136961

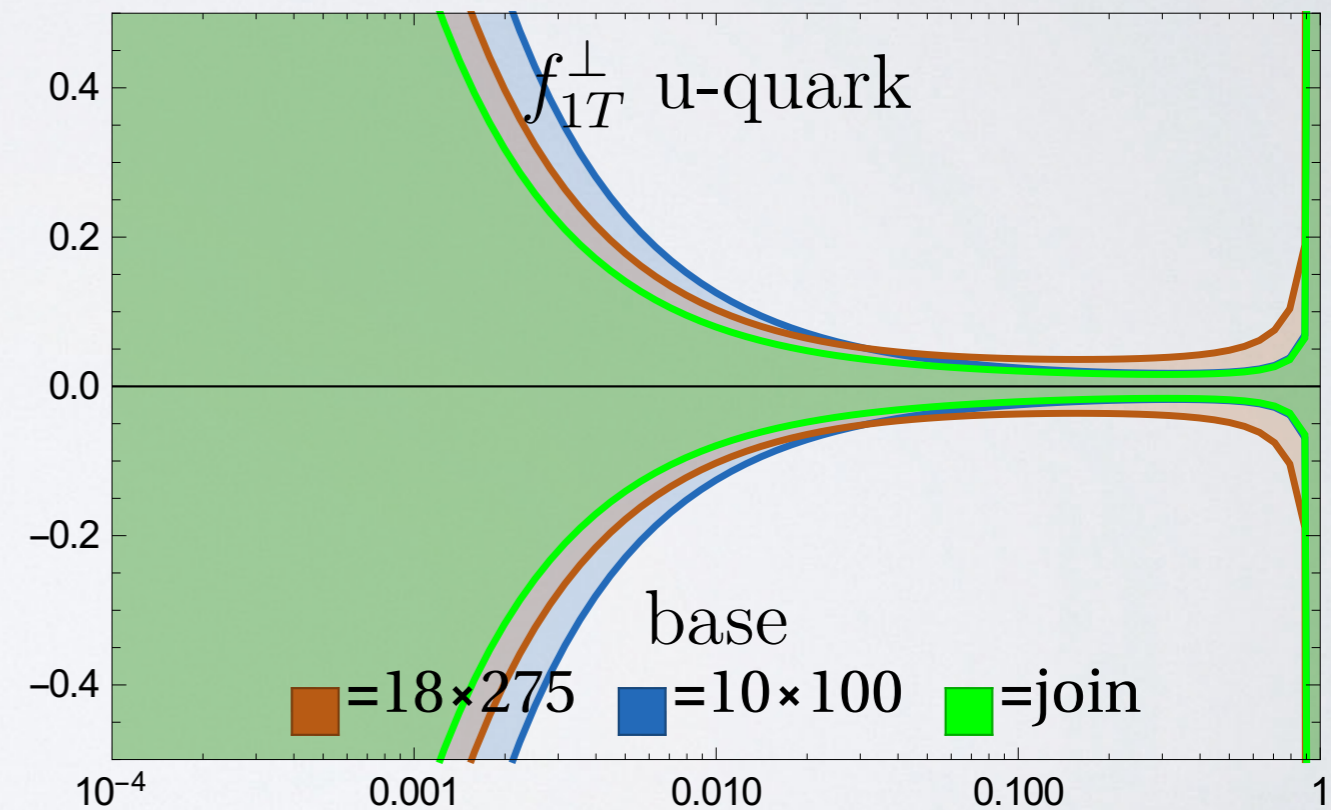


Fig.26 of the paper x

EIC impact on Sivers TMD

TSSA $e p^\uparrow \rightarrow e' + \pi^+ + X$

Adam et al. (ATHENA Coll.), JINST 17 (22) P10019

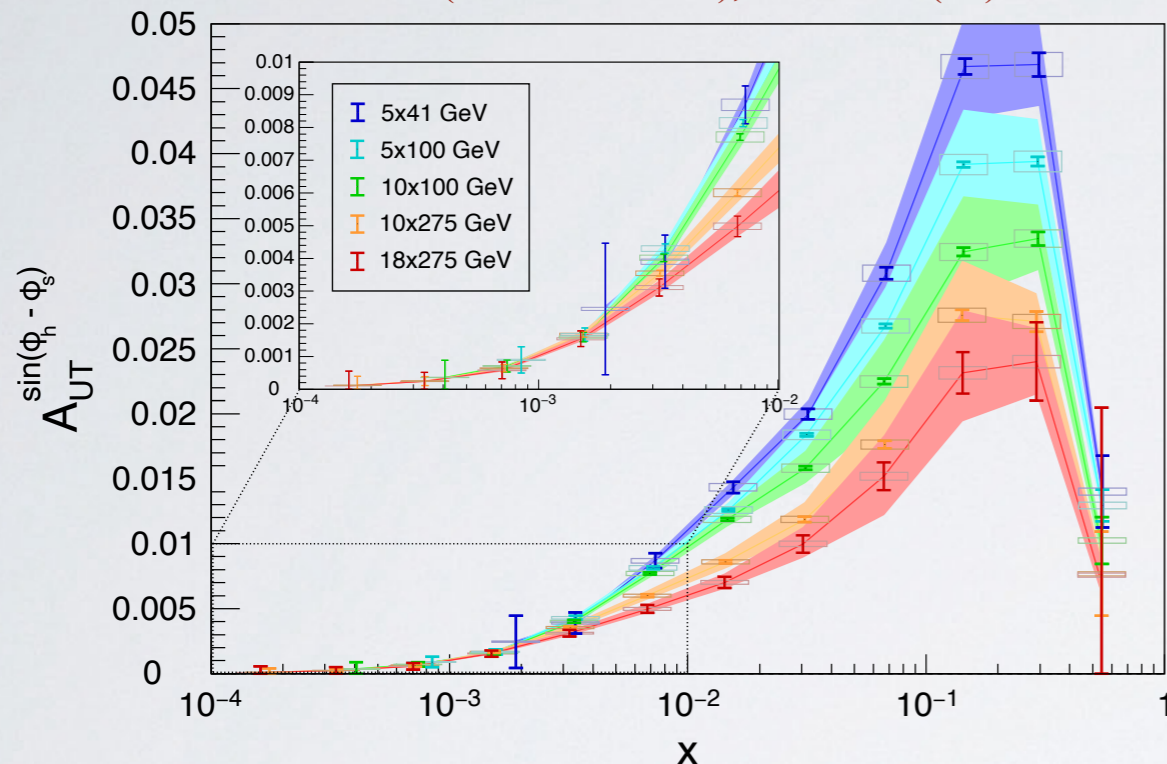


Fig.18 of the paper

Sivers TMD from

Bacchetta et al., P.L. B827 (22) 136961

At $x \sim 0.1$ larger impact from medium energy configuration

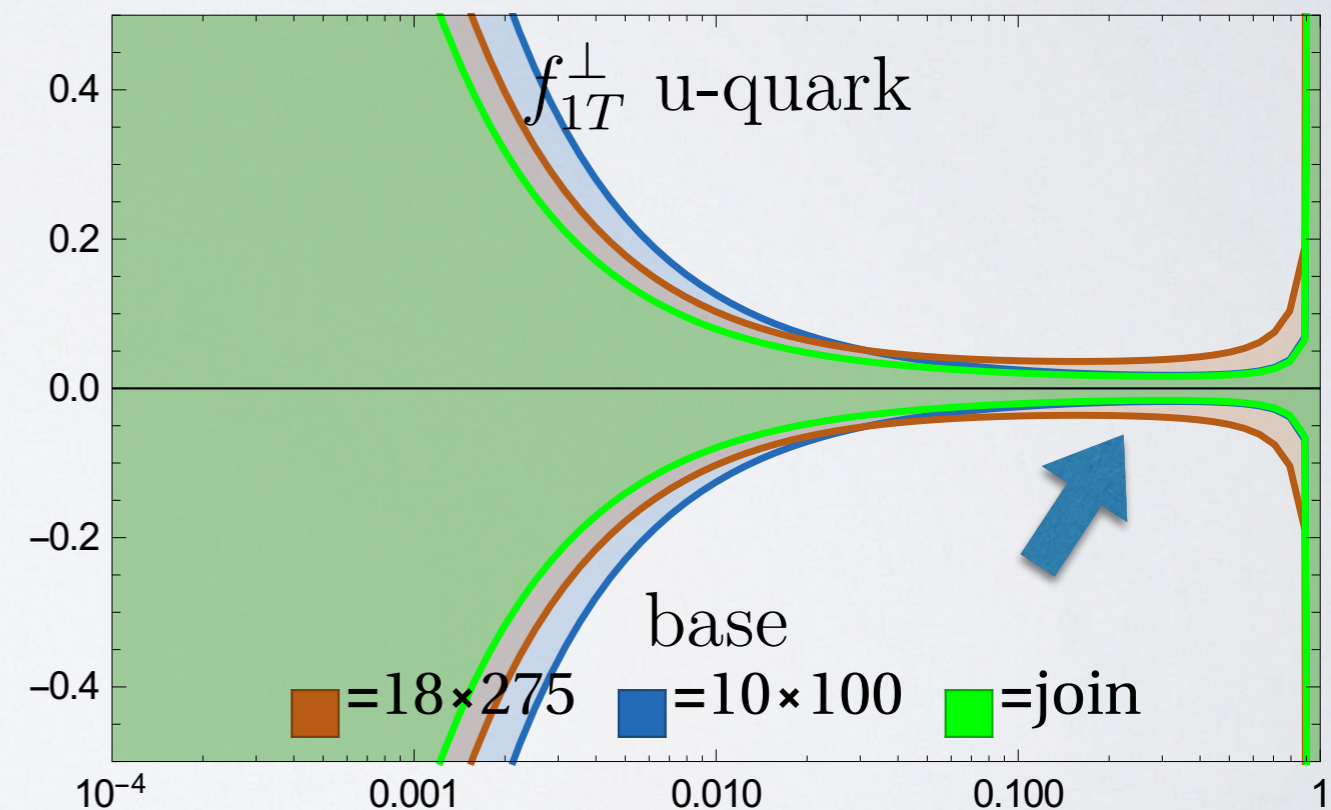
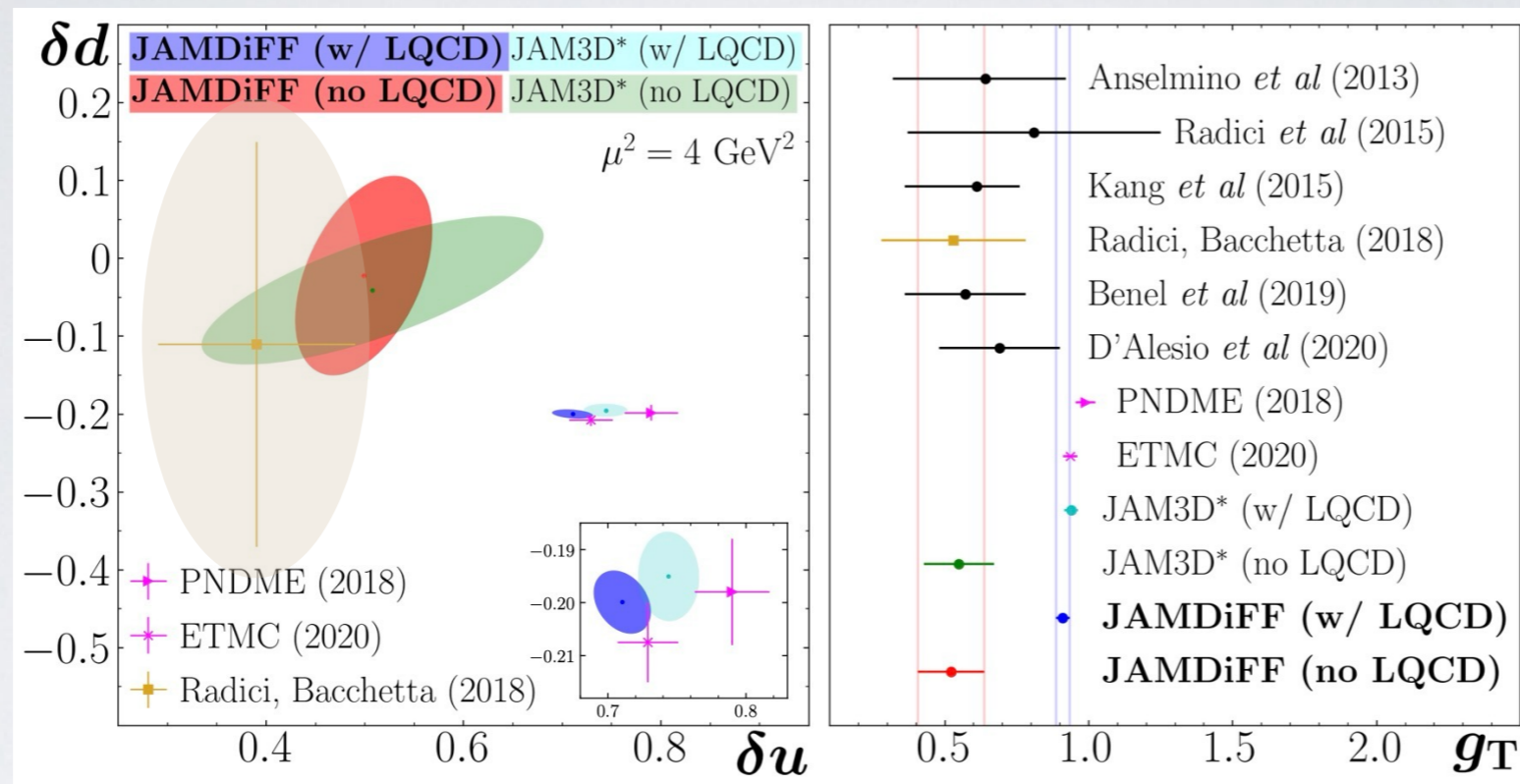


Fig.26 of the paper \mathcal{X}

Tensor charge: tension pheno-lattice

$$\delta q(Q^2) = \int_0^1 dx h_1^{q-\bar{q}}(x, Q^2)$$

$$g_T = \delta u - \delta d$$



adapted from D. Pitonyak, QCD Evolution 24

- **approximate compatibility of JAM with other phenomenology** when using both Collins effect and di-hadron mechanism but **not including lattice** results in the fit
- **including lattice as prior**, JAM still compatible with exp. data with both Collins effect and di-hadron mechanism but **deviates from other phenomenology**

EIC impact on tensor charge

Gamberg *et al.*, P.L. **B816** (21)

Collins effect

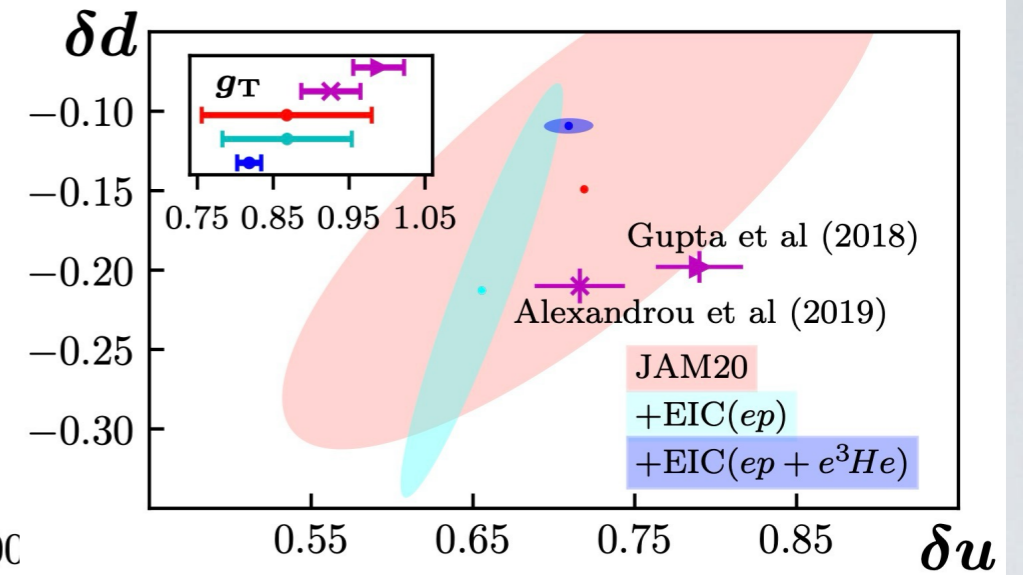
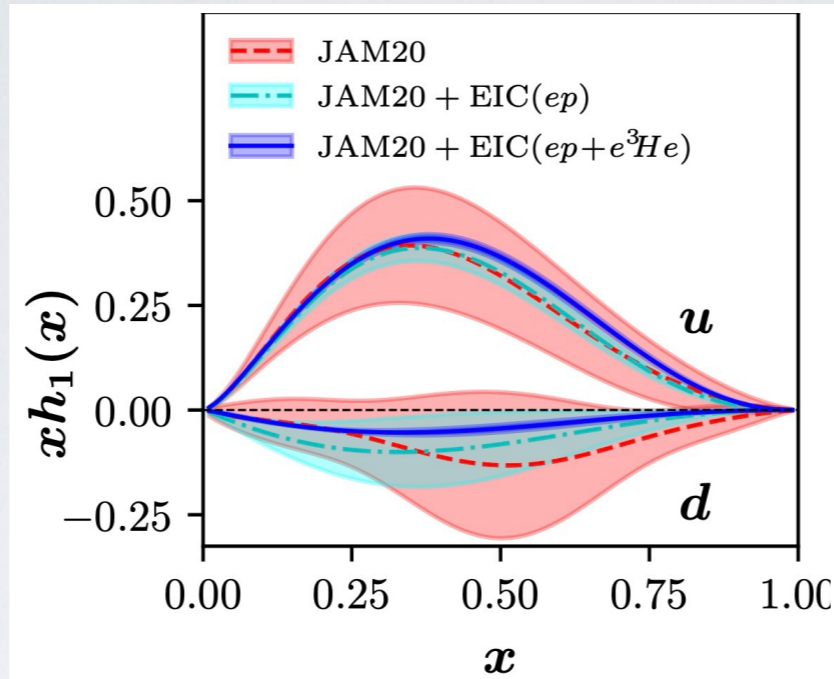
$\mathcal{L}=10 \text{ fb}^{-1}$, 8223 data pts.

proton [GeV]:

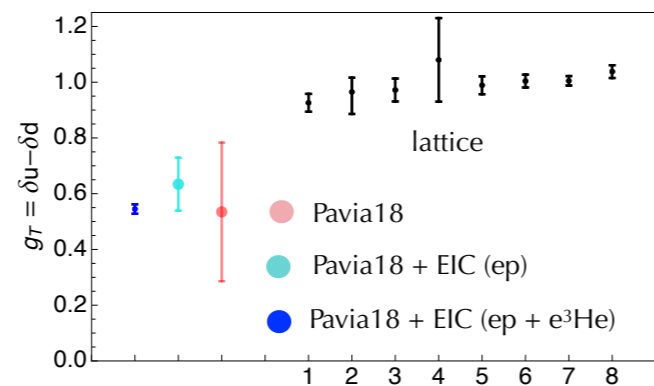
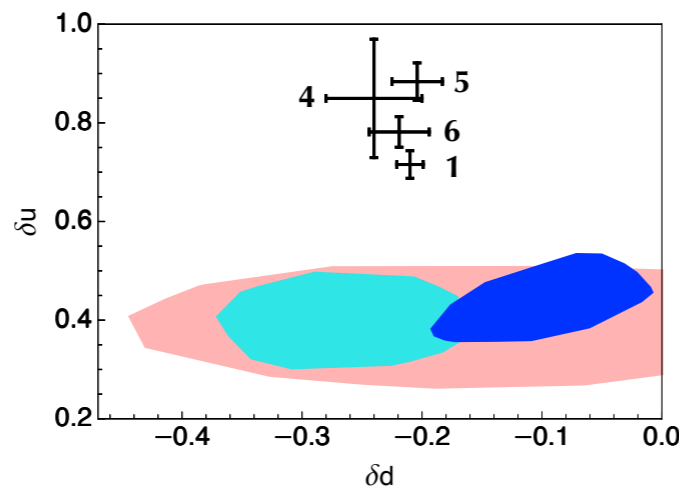
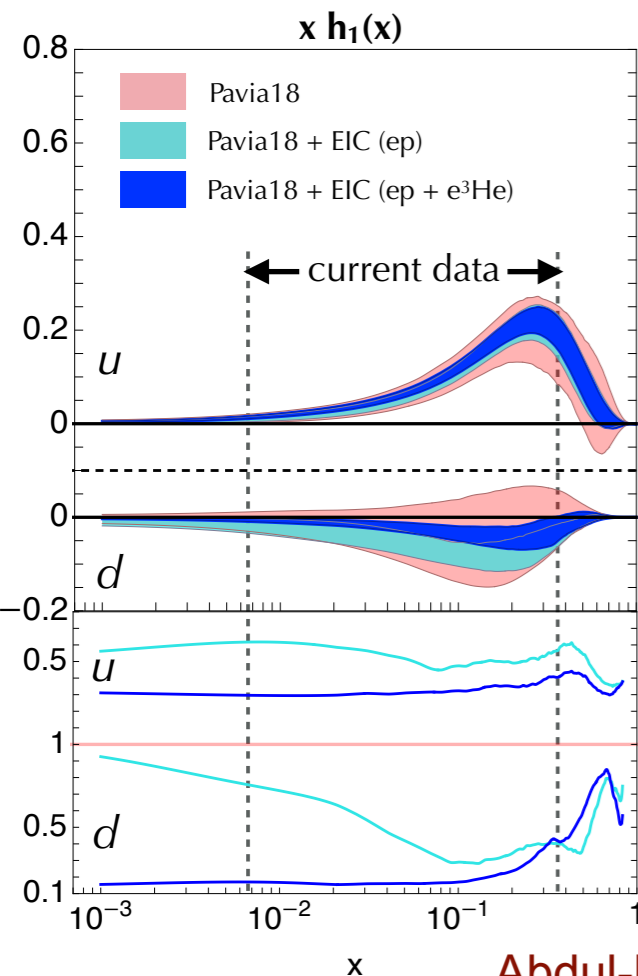
5x41, 5x100, 10x100, 18x275

^3He [GeV]:

5x41, 5x100, 18x100



2



Abdul-Khalek *et al.* (EIC Yellow Report),
N.P. **A1026** (22) 122447

di-hadron mechanism

$\mathcal{L}=10 \text{ fb}^{-1}$, 3852 data pts

proton & ^3He [GeV]: 10x100

Lattice results

- 1) ETMC '19 [Alexandrou et al., arXiv:1909.00485](#)
- 2) Mainz '19 [Harris et al., P.R. D100 \(19\) 034513](#)
- 3) LHPC '19 [Hasan et al., P.R. D99 \(19\) 114505](#)
- 4) JLQCD '18 [Yamanaka et al., P.R. D98 \(18\) 054516](#)
- 5) PNDME '18 [Gupta et al., P.R. D98 \(18\) 034503](#)
- 6) ETMC '17 [Alexandrou et al., P.R. D95 \(17\) 114514; \(E\) P.R. D96 \(17\) 099906](#)
- 7) RQCD '14 [Bali et al., P.R. D91 \(15\) 054501](#)
- 8) LHPC '12 [Green et al., P.R. D86 \(12\) 114509](#)



EIC impact on tensor charge

Gamberg *et al.*, P.L. **B816** (21)

Collins effect

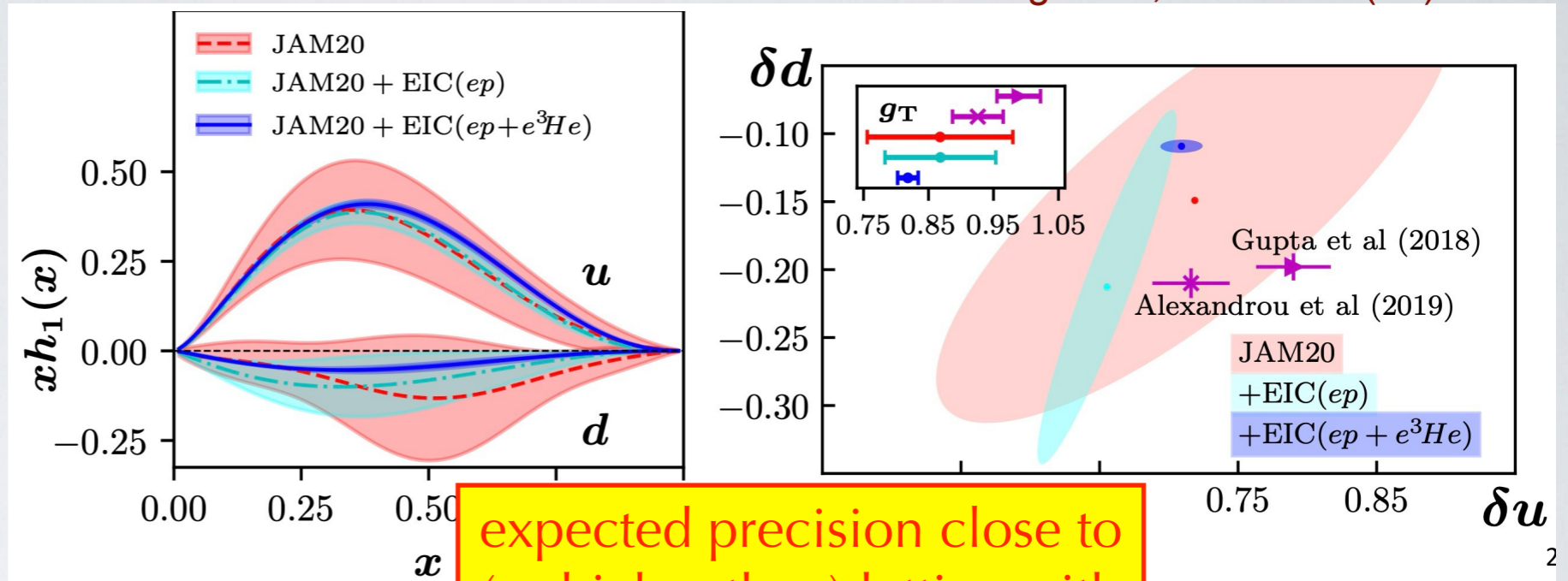
$\mathcal{L}=10 \text{ fb}^{-1}$, 8223 data pts.

proton [GeV]:

5x41, 5x100, 10x100, 18x275

^3He [GeV]:

5x41, 5x100, 18x100



expected precision close to (or higher than) lattice with just $\sqrt{s} \sim 63 \text{ GeV}$

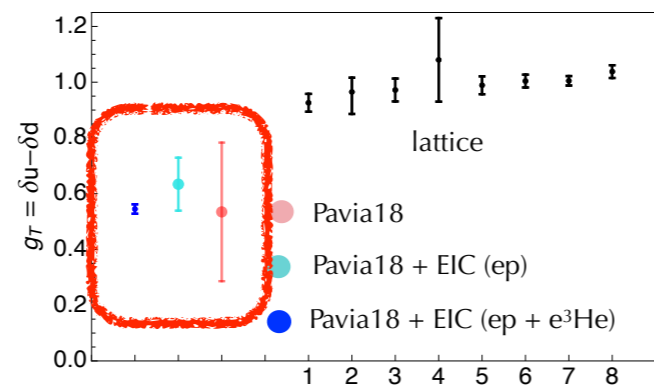
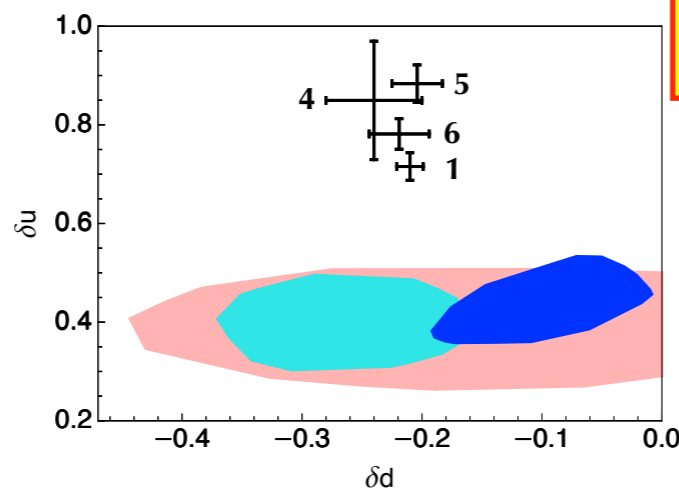
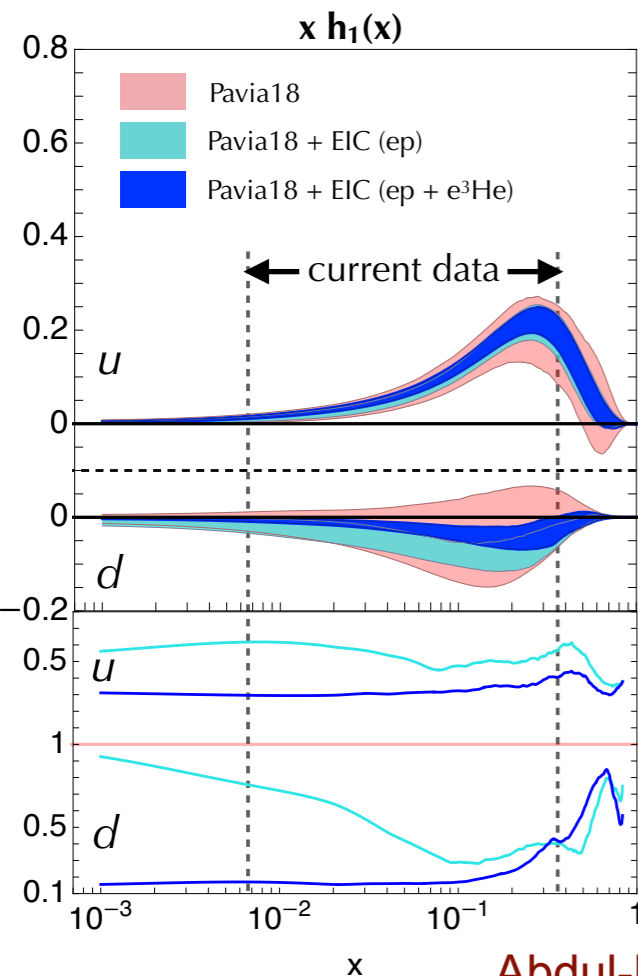
di-hadron mechanism

$\mathcal{L}=10 \text{ fb}^{-1}$, 3852 data pts

proton & ^3He [GeV]: 10x100

Lattice results

- 1) ETMC '19 Alexandrou et al., arXiv:1909.00485
- 2) Mainz '19 Harris et al., P.R. D100 (19) 034513
- 3) LHPC '19 Hasan et al., P.R. D99 (19) 114505
- 4) JLQCD '18 Yamanaka et al., P.R. D98 (18) 054516
- 5) PNDME '18 Gupta et al., P.R. D98 (18) 034503
- 6) ETMC '17 Alexandrou et al., P.R. D95 (17) 114514; (E) P.R. D96 (17) 099906
- 7) RQCD '14 Bali et al., P.R. D91 (15) 054501
- 8) LHPC '12 Green et al., P.R. D86 (12) 114509



Abdul-Khalek *et al.* (EIC Yellow Report), N.P. **A1026** (22) 122447

The reference paper

Precision Studies of QCD in the Low Energy Domain of the EIC

V.D. Burkert,¹ L. Elouadrhiri,¹ A. Afanasev,² J. Arrington,³ M. Contalbrigo,⁴ W. Cosyn,^{5,6} A. Deshpande,⁷ D.I. Glazier,⁸ X. Ji,^{9,10} S. Liuti,¹¹ Y. Oh,^{12,13} D. Richards,¹ T. Satogata,¹ A. Vossen,^{14,1} H. Abdolmaleki,¹⁵ A. Albataineh,¹⁶ C.A. Aidala,¹⁷ C. Alexandrou,¹⁸ H. Avagyan,¹ A. Bacchetta,¹⁹ M. Baker,¹ F. Benmokhtar,²⁰ J.C. Bernauer,^{7,21} C. Bissolotti,¹⁹ W. Briscoe,² D. Byers,¹⁴ Xu Cao,²² C.E. Carlson,²³ K. Cichy,²⁴ I.C. Cloet,²⁵ C. Cocuzza,²⁶ P.L. Cole,²⁷ M. Constantinou,²⁶ A. Courtoy,²⁸ H. Dahiya,²⁹ K. Dehmelt,⁷ S. Diehl,^{30,31} C. Dilks,¹⁴ C. Djalali,³² R. Dupré,³³ S.C. Dusa,¹ B. El-Bennich,³⁴ L. El Fassi,³⁵ T. Frederico,³⁶ A. Freese,³⁷ B.R. Gamage,¹ L. Gamberg,³⁸ R.R. Ghoshal,¹ F.X. Girod,¹ V.P. Goncalves,^{39,22,40} Y. Gotra,¹ F.K. Guo,^{41,42} X. Guo,⁹ M. Hattawy,⁴³ Y. Hatta,⁴⁴ T. Hayward,³⁰ O. Hen,⁴⁵ G. M. Huber,⁴⁶ C. Hyde,⁴³ E.L. Isupov,⁴⁷ B. Jacak,³ W. Jacobs,⁴⁸ A. Jentsch,⁴⁴ C.R. Ji,⁴⁹ S. Joosten,²⁵ N. Kalantarians,⁵⁰ Z. Kang,^{51,52,53} A. Kim,^{30,1} S. Klein,³ B. Kriesten,¹⁰ S. Kumano,⁵⁴ A. Kumar,⁵⁵ K. Kumericki,⁵⁶ M. Kuchera,⁵⁷ W.K. Lai,^{58,59,51} Jin Li,⁶⁰ Shujie Li,³ W. Li,⁶¹ X. Li,⁶² H.-W. Lin,⁶³ K.F. Liu,⁶⁴ Xiaohui Liu,^{65,66} P. Markowitz,⁵ V. Mathieu,^{67,68} M. McEneaney,¹⁴ A. Mekki,⁶⁹ J.P. B. C. de Melo,⁷⁰ Z.E. Meziani,²⁵ R. Milner,⁴⁵ H. Mkrtychyan,⁷¹ V. Mochalov,^{72,73} V. Mokeev,¹ V. Morozov,⁷⁴ H. Moutarde,⁷⁵ M. Murray,⁷⁶ S. Mtingwa,⁷⁷ P. Nadel-Turonski,⁵³ V.A. Okorokov,⁷³ E. Onyie,¹ L.L. Pappalardo,^{4,78} Z. Papandreou,⁷⁹ C. Pecar,¹⁴ A. Pilloni,^{80,81} B. Pire,⁸² N. Polys,⁸³ A. Prokudin,^{84,1} M. Przybycien,⁸⁵ J.-W. Qiu,¹ M. Radici,⁸⁶ R. Reed,⁸⁷ F. Ringer,^{1,43} B.J. Roy,⁸⁸ N. Sato,¹ A. Schäfer,⁸⁹ B. Schmookler,⁹⁰ G. Schnell,⁹¹ P. Schweitzer,³⁰ R. Seidl,^{92,21} K.M. Semenov-Tian-Shansky,^{12,93,94} F. Serna,^{95,96} F. Shaban,⁹⁷ M.H. Shabestari,⁹⁸ K. Shiells,¹⁰ A. Signori,^{99,100} H. Spiesberger,¹⁰¹ I. Strakovsky,² R.S. Sufian,^{23,1} A. Szczepaniak,^{102,1} L. Teodorescu,¹⁰³ J. Terry,^{51,52} O. Teryaev,¹⁰⁴ F. Tessarotto,¹⁰⁵ C. Timmer,¹ Abdel Nasser Tawfik,¹⁰⁶ L. Valenzuela Cazares,¹⁰⁷ A. Vladimirov,^{89,108} E. Voutier,³³ D. Watts,¹⁰⁹ D. Wilson,¹¹⁰ D. Winney,^{111,112} B. Xiao,¹¹³ Z. Ye,¹¹⁴ Zh. Ye,¹¹⁵ F. Yuan,³ N. Zachariou,¹⁰⁹ I. Zahed,⁷ J.L. Zhang,⁶⁰ Y. Zhang,¹ and J. Zhou¹¹⁶

Prog. Part. Nucl. Phys. 131 (2023) 104032, arXiv:2211.15746

Invite all of you to read it !

